The value of ASCAT soil moisture and MODIS snow cover data for calibrating a conceptual hydrologic model

Rui Tong[1,2], Juraj Parajka[1,2], Andreas Salentinig[3], Isabella Pfeil[1,3], Jürgen Komma[2], Borbála Széles[1,2], Martin Kubáň[4], Peter Valent[2,4], Mariette Vreugdenhil[3], Wolfgang Wagner[1,3] and Günter Blöschl[1,2]

[1]Centre for Water Resource Systems, TU Wien, Vienna, 1040, Austria
[2]Institute of Hydraulic Engineering and Water Resources Management, TU Wien, Vienna, 1040, Austria
[3]Department of Geodesy and Geoinformation, TU Wien, Vienna, 1040, Austria
[4]Department of Land and Water Resources Management, Slovak University of Technology, Bratislava, 810 05, Slovakia

Correspondence to: Rui Tong (tong@hydro.tuwien.ac.at)

Abstract. Recent advances in soil moisture remote sensing have produced satellite datasets with improved soil moisture mapping under vegetation and with higher spatial and temporal resolutions. In this study, we evaluate the potential of a new, experimental version of the ASCAT Soil Water Index dataset for multiple objective ~~calibration~~calibrations of a conceptual hydrologic model. The analysis is performed in 213 catchments in Austria for the period 2000-2014. An HBV type hydrologic model is calibrated to runoff data, ASCAT soil moisture data, and MODIS snow cover data for various calibration variants. Results show that the inclusion of soil moisture data in the calibration mainly improves the soil moisture simulations; the inclusion of snow data mainly improves the snow simulations~~;~~, and including both of them improves both soil moisture and snow simulations to almost the same extent. The snow data are more efficient in improving snow simulations than the soil moisture data are in improving soil moisture simulations. The improvements of both runoff and soil moisture model efficiencies are larger in low elevation and agricultural catchments than in others. The calibrated snow-related parameters are strongly affected by including snow data, and to a lesser extent by soil moisture data~~, while~~. In contrast, the soil-related parameters are only affected by the inclusion of soil moisture data.

1 Introduction

Estimating the spatial and temporal variability of water balance components at the regional scale is important for solving a range of practical issues in water resources management and planning, as well as for understanding catchment functioning in terms of how runoff generation processes interact to produce catchment response. One estimation approach is by hydrologic models. There is a variety of model types and model parameters estimation methods. Notwithstanding their usefulness, the resulting simulations of the water balance components are subject to uncertainty due to uncertainty in model inputs, parameter estimation and model structure (Kavetski et al., 2006; Parajka et al., 2007; Wagener and Montanari, 2011).

Previous studies have demonstrated that multiple objective calibration helps to constrain hydrologic models and hence to reduce uncertainty and to improve predictions in hydrological modelling (e.g. Efstratiadis and Koutsoyiannis, 2010). Most of these studies examined the value of constraining hydrologic models by combining different runoff signatures (e.g. by simultaneous calibration of the models to low and high flows or timing) or calibrating hydrologic models to runoff and some additional hydrological variable such as snow cover (e.g. Udnæs et al., 2007; Parajka and Blöschl, 2008; Franz and Karsten, 2013; Duethmann et al., 2014; Finger et al., 2015, Han et al., 2019, Sleziak et al., 2020), soil moisture (e.g. Parajka et al., 2009; Sutanudjaja et al., 2014; Wanders et al., 2014; Rajib et al., 2016; Kundu et al., 2017, Li et al., 2018), evaporation (e.g. Immerzeel and Droogers, 2008; Zhang et al., 2009), groundwater level data (Seibert, 2000) or total water storage (e.g. Lo et al., 2010; Werth and Güntner, 2010; Rakovec et al., 2016; Bai et al., 2018; Trautmann et al., 2018). These studies showed that the use of additional information typically improves the spatial and/or temporal patterns of internal state variables and fluxes, but does not necessarily improve the efficiency of simulating runoff. Most of the studies reported a small degradation of runoff model efficiency while the internal consistency of the models has been improved. A few studies also tested the combination of more variables in multiple objective calibration (e.g. Milzow et al., 2011; Kunnath-Poovakka et al., 2016; López et al., 2017; Nijzink et al., 2018; Demirel et al., 2019; Szeles et al., ~~2020a,b~~2020, 2021) and found that the combination of different variables generally reduced the parameter uncertainty particularly in data poor regions. For example, Nijzink et al. (2018) ~~also~~ demonstrated that constraining hydrologic models profited from an increased number of data sources. Interestingly, ~~combining~~the use of different soil moisture ~~and satellite~~ products had a positive impact on the identifiability of not only soil but also snow model parameters.

The factors that control these improvements are less well understood. Snow cover data improved snow and runoff simulations in small catchments without precipitation observations (Parajka and Blöschl, 2008~~) and~~). They helped to reduce snow underestimation errors in flatland catchments in changing climate conditions (Sleziak et al., 2020). Including evapotranspiration estimates improved regionalization and simulations of daily and monthly runoff particularly in drier regions with lower runoff volumes. (Zhang et al., 2009). The use of total water storage data from GRACE improved runoff simulations on monthly or longer time scales, particularly in wet catchments (Rakovec et al. 2016). Only a few studies examined the factors that control the changes in efficiency when using soil moisture information (Rajib, et al., 2016). Parajka et al., (2006) showed that soil moisture efficiency of a model calibrated to runoff and satellite soil moisture was lower in hilly and alpine regions with large topographical variability as compared to the flatlands. Nijzink et al. (2018) reported that the AMSR-E soil moisture product improved the identifiability of model parameters in peaty lowland catchments.

Recent advances in the observation techniques of soil moisture, particularly in passive and active microwave remote sensing, increases the availability of regional and global soil moisture datasets (Babaeian et al., 2019). Passive microwave sensors operating in the 1-10 GHz frequency range suitable for soil moisture retrieval include the L-band radiometers flown on board the Soil Moisture Active Passive (SMAP) and Soil Moisture and Ocean Salinity (SMOS) missions, and the multi-frequency radiometer Advanced Microwave Scanning Radiometer 2 (AMSR-2). In the active domain, soil moisture retrievals from the C-band Advanced Scatterometer (ASCAT) have found widespread use in geoscientific applications (Brocca et al. 2017). All

these satellites have a rather coarse spatial resolution in the order of tens of kilometres (10-50 km). Various validation studies have shown that ASCAT soil moisture data sets (Wagner et al. 2013) are less accurate than corresponding SMAP soil moisture data sets (Kim et al. 2020) but, overall, comparable in quality with SMOS and AMSR-2 (Chen et al., 2018; El Hajj et al., 2018; Mousa and Shu 2020). Nonetheless~~,~~ there are important regional differences in the quality of the satellite soil moisture data sets, with ASCAT performing in general poorest over arid environments and best over more densely vegetated regions. Over the United States and Europe, comparisons with in-situ soil moisture data from dense networks have revealed the presence of seasonal biases in the ASCAT soil moisture time series (Wagner et al., 2014). Pfeil et al. (2018) and Hahn et al. (2020) have demonstrated that these seasonal biases can be much reduced by enhancing the vegetation parameterization of the TU Wien change detection model introduced by Wagner et al. (1999). The launch of the Sentinel-1 series provides observations at a high spatial resolution of 5x20 m. Over mountainous environments, soil moisture retrievals from all microwave sensors are in general much less reliable than over flatland regions due to significant topographic variations within the coarse-resolution satellite footprints and the presence of rocks, ice, snow, and dense vegetation. Nonetheless, in the snow- and frost-free summer months, the satellite retrievals may have some skill as demonstrated by Brocca et al. (2013) for an alpine catchment in northern Italy.

The objective of this study is to test the value of a new ASCAT Soil Water Index (SWI) data product for multiple objective calibration and validation of a conceptual hydrologic model. Compared to the operational ASCAT SWI product as distributed by the Copernicus Global Land Service, this experimental SWI data product mainly benefits from a new vegetation parameterization of the ASCAT surface soil moisture retrieval algorithm and an improved spatial representation due to the application of a new directional resampling method based on Sentinel-1 Synthetic Aperture Radar (SAR) data. The main aims are: (1) to evaluate the performance of a conceptual hydrologic model calibrated to satellite soil moisture and runoff ~~and~~, (2) to test the impact of weight on the runoff objective in model calibration, (~~2~~3) to compare the multiple objective calibration to soil moisture and runoff to three different calibration variants – (i) traditional calibration to runoff only, (ii) multiple objective calibration to satellite snow cover and runoff and (iii) multiple objective calibration to satellite snow cover, soil moisture and runoff; (~~3~~4) to examine factors which control the model performance at the regional scale. The analysis is performed by confronting a conceptual hydrologic model with ASCAT SWI soil moisture data for 213 catchments in Austria, which represent a wide range of physiographic settings typical of Central European conditions.

2 Data

2.1 ASCAT Soil Water Index product

For producing a new, experimental version of the ASCAT Soil Water Index (SWI) data set, we deployed the same algorithms as used within the EUMETSAT H SAF and Copernicus Global Land Service~~, but with~~. The novelty is the application of a new parameterization for the vegetation correction (Hahn et al., 2020) and a new approach for disaggregating the ASCAT soil

moisture retrievals to a finer grid~~, which~~. This approach is currently under review by H SAF for producing the planned Metop ASCAT Disaggregated Surface Soil Moisture Near Real Time 1 km sampling (ASCAT DIS SSM NRT 1 km - H28) data product~~.~~.. The main steps in the processing are: (i) retrieving surface soil moisture from ASCAT backscatter time series using the TU Wien change detection algorithm adopted to ASCAT (Naeimi et al., 2009) and using the vegetation parameterization as recommended by Pfeil et al. (2018), (ii) disaggregating the ASCAT surface soil moisture data to a regular 500 m grid using the directional resampling method as described in the Algorithm Theoretical Baseline Document (ATBD) for the planned H SAF H28 data product, and (iii) computing the Soil Water Index (SWI) using the iterative implementation of the exponential filter introduced by Wagner et al. (1999) and Albergel et al. (2008) with a characteristic time value of T = 10 days, representing root zone soil moisture. This last processing step makes the ASCAT soil moisture data better comparable to the modelled soil moisture data as it filters out high-frequency fluctuations of the ASCAT surface soil moisture retrievals and samples the data at regular time intervals. The disaggregation step is based on the analysis of Sentinel 1 backscatter time series sampled to 500 m~~, and essentially looks~~. It essentially looks for the best direction from which the ASCAT data are interpolated to the 500 m grid. Thereby it improves the resampling especially near large lakes or near large urban areas. To exclude invalid ASCAT measurements of snow and frozen ground, soil moisture was masked using soil temperature and snow cover from ECMWF Copernicus Climate Service (C3S) ERA5-Land. Soil moisture was masked when soil temperatures at a soil depth of 0-7 cm were below 1°C or snow cover exceeded 30 % of the pixel.

2.2 MODIS snow cover product

Snow cover is mapped by combining the MODIS products from the Terra (MOD10A1) and Aqua (MYD10A1) satellites (Hall and Riggs, 2016a, b). Version 6 of the MOD10A1 and MYD10A1 datasets ~~provides~~provide daily maps of Normalized Difference Snow Index (NDSI) at a 500 m spatial resolution. The NDSI values range between 0.0 and 1.0, and snow cover is considered to be present if NDSI is larger than a threshold. Former MODIS versions used a fixed threshold (0.4), but Tong et al. (2019) found that in Austria, this threshold can be seasonally optimized for different altitudes and land cover classes. In this study, we use a threshold that varies seasonally, decreases with increasing elevation and is lower in forested than open land cover settings (see supplementary Table ~~1~~S1). Such a varying threshold improves the regional snow cover mapping by 3-10%, mainly in forested regions above 900m a.s.l. (Tong et al., ~~2019~~2020). The classified snow cover maps from Terra and Aqua are then combined to reduce the effect of clouds. Pixels classified as clouds or missing in Terra are replaced by pixels from Aqua if these are classified as snow--covered or snow--free (Parajka and Blöschl, 2008).

2.3 Study area and other data

The value of satellite data for the calibration of hydrologic models is evaluated in 213 catchments in Austria (Figure 1, Table ~~2~~1). This set of catchments has been selected in previous studies (Viglione et al., 2013, Sleziak et al., 2020) to represent diverse physiographic, landscape and hydrologic characteristics which are not significantly affected by human impact. Selected

catchment characteristics of this dataset are presented in Table ~~2~~1. The size of the catchments varies from 13.7 to 6214 km^2, and their mean elevation ranges from 353 m a.s.l. to 2940 m a.s.l.. Topographical characteristics are derived from a digital elevation model with 500m spatial resolution. Land cover in Austria is mainly agricultural crops and meadows in the lowlands and forest in the medium elevation ranges. Alpine vegetation and rocks prevail in catchments in the Alps. Land cover characteristics are derived from the CORINE land cover mapping (CLC2006 dataset, EEA, 2013, https://land.copernicus.eu~~/~~/), and Normalized Difference Vegetation Index (MOD13A3v006) is generated from MODIS C6 1km monthly data (Didan, 2015). Austria has a warm temperate climate, except ~~of~~for the Alps. The largest precipitation rates (more than 2000 mm/year) occur in the west, mainly due to orographic lifting of northwesterly airflows at the rim of the Alps. Mean annual catchment precipitation is lower (less than 800mm/year) in the lowlands in the east, and the contrast with the Alps is reinforced by the higher air temperature and much higher evaporation in the lowlands. Soil characteristics are derived from a 1km global map of soil hydraulic properties (Zhang et al., 2018). This dataset provides the mean and standard deviations of selected soil hydraulic parameters based on the Kosugi water retention model (Kosugi 1994, 1996) at a 1 km resolution for surface soils (0-5cm).

Hydrological and meteorological data are obtained from Central Hydrographical Bureau (HZB, ehyd.gv.at) and Zentralanstalt für Meteorologie und Geodynamik (ZAMG). Model inputs (i.e. mean daily precipitation and air temperature) are derived from the gridded SPARTACUS dataset (Hiebl and Frei, 2016, 2018). This dataset provides long-term daily gridded (1km spatial resolution) maps which are consistently interpolated by using a consistent station network throughout the entire period (Duethmann et al., 2020). Mean daily potential evaporation is derived from gridded maps of mean daily air temperature and potential sunshine duration index by using a modified Blaney–Criddle approach (Parajka et al., 2003). Daily runoff data from 213 catchments are used for calibrating and 208 catchments for validating the hydrologic model.

The precipitation, air temperature, runoff and MODIS snow cover data are available from September 2000 to August 2014. The ~~concurrent~~concurrently available period for the soil moisture ASCAT SWI data is January 2007 to August 2014.

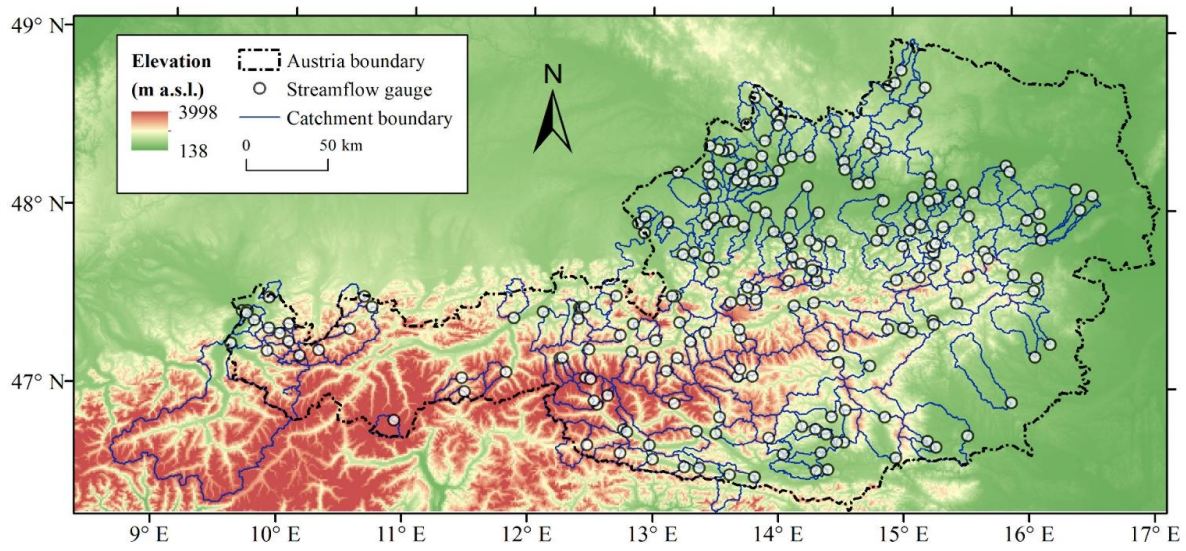

Figure 1: Topography of Austria and the location of the 213 catchments.

3 Methods

3.1 Conceptual hydrologic model

The hydrologic model used in this study is a semi-distributed version of TUW model, following the structure of the HBV model (Bergström 1992; Parajka et al., 2007). A simple illustration of the model structure is presented in Figure 2. The model consists of three routines, i.e. snow accumulation and melt, soil moisture accounting and runoff routine. The snow part has five model parameters and is based on a simple degree-day method: the snow correction factor SCF to account for errors in measurement of snowfall due to gauge undercatch, the degree–day factor DDF, and three threshold temperatures Ts, Tr, meltT. The soil moisture routine has three parameters: the maximum soil moisture storage in the root zone FC, a limit that controls the actual evapotranspiration LP and a nonlinear parameter for runoff production beta. The routing involves two parts, within-catchment routing and stream routing. The within-catchment routing has five parameters: three storage coefficient k0, k1 and k2 for three conceptual reservoirs representing overland flow, interflow and base flow, a threshold for very fast response lsuz and a constant percolation rate cperc connecting the fast and slow reservoirs. The stream routing uses a triangular transfer function with two parameters: bmax and croute. The total number of model parameters that are calibrated is 15 (Table ~~3~~2). The model is run in a semi-distributed way, i.e. model inputs and outputs are estimated for elevation zones of 200m while the model parameters are assumed to be lumped (i.e. constant) in each catchment. In order to match the model simulations to the dimensionless satellite soil water index, the simulated soil moisture is scaled by the field capacity (i.e. the- model parameter FC), to obtain a relative root zone moisture ranging from 0 to 1. More details about the model can be found in the Appendix of Parajka et al. (2007).

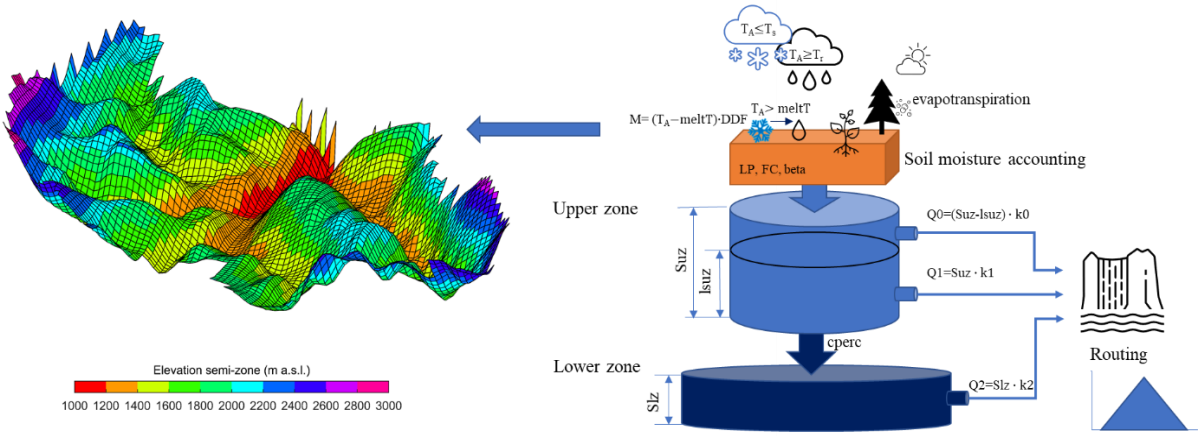

Figure 2: Conceptual description of TUWmodel structure.

3.2 Multiple objective calibration and validation of hydrologic model

The value of using satellite soil moisture (SSM) data for multiple objective calibration of conceptual hydrologic models is compared to three other calibration variants: (1) traditional calibration to runoff only, (2) multiple objective calibration to satellite snow cover (SSC) and runoff and (3) multiple objective calibration to SSM, SSC and runoff. The general form of the calibration objective function F used in this study consists of minimizing the weighted sum of individual objectives related to runoff (O_Q), soil moisture (O_{SM}) and snow cover (O_{SC}):

$$F = w_Q \cdot O_Q + w_{SM} \cdot O_{SM} + w_{SC} \cdot O_{SC} \qquad (1)$$

where w_Q, w_{SM} and w_{SC} are the weights of the respective objectives. In each multiple objective calibration variant, 11 runoff weights (from 0.0 to 1.0 with a step of 0.1) are tested (Table 43). The soil moisture and snow weights are assumed to be equal for symmetry, and are calculated by setting the sum of all weights to 1.0.

The individual objectives O_Q, O_{SM} and O_{SC} are defined as follows. The runoff objective O_Q consists of a combination of two variants of the Nash-Sutcliffe coefficient *NSE* and NSE_{log} (Nash and Sutcliffe, 1970):

$$O_Q = 0.5 \cdot NSE + 0.5 \cdot NSE_{log} \qquad (2)$$

$$NSE = 1 - \frac{\sum_{i=1}^{n}\left(Q_{obs,i} - Q_{sim,i}\right)^2}{\sum_{i=1}^{n}\left(Q_{obs,i} - \overline{Q_{obs}}\right)^2} \qquad (3)$$

$$NSE_{\log} = 1 - \frac{\sum_{i=1}^{n}\left(\log(Q_{obs,i}) - \log(Q_{sim,i})\right)^2}{\sum_{i=1}^{n}\left(\log(Q_{obs,i}) - \log(\overline{Q_{obs}})\right)^2} \qquad (4)$$

where $Q_{obs,i}$ and $Q_{sim,i}$ represent observed and simulated daily runoff of day i, respectively and Q_{obs} is the average of observed daily runoff over the calibration (or verification) period of n days. The choice of the equal weighting of NSE and NSE_{log} is based on previous studies in the study region (e.g. Parajka and Blöschl, 2008) to emphasize both the high and low flow conditions.

The soil moisture objective function (O_{SM}) is expressed by the correlation coefficient r between relative soil moisture estimated from the ASCAT and simulated by the hydrologic model:

$$O_{SM} = \frac{\sum_{i=1}^{n}\left((\theta_{sim,i} - \overline{\theta_{sim}})(\theta_{obs,i} - \overline{\theta_{obs}})\right)}{\sqrt{\sum_{i=1}^{n}\left((\theta_{sim,i} - \overline{\theta_{sim}})^2(\theta_{obs,i} - \overline{\theta_{obs}})^2\right)}} \qquad (5)$$

where θ_{sim} is the relative root zone soil moisture simulated by the model and θ_{obs} is the ASCAT SWI. The correlation coefficient is selected as a measure of similarity because it allows a comparison of the temporal dynamics irrespective of the respective magnitudes and possible intercepts in the relationship between observed and simulated soil moisture.

The snow cover objective function O_{SC} involves the sum of snow overestimation S_O and underestimation S_U errors:

$$O_{SC} = 1 - (S_O + S_U) \qquad (6)$$

The estimation of S_O and S_U follows the strategy proposed and evaluated in Parajka and Blöschl (2008). The snow overestimation error indicates the relative number of days when the hydrologic model simulates snow but the satellite (MODIS) does not observe snow cover:

$$S_O = \frac{1}{\sum_{i=1}^{N_{days}}\sum_{j=1}^{N_{zones}} A_{i,j}} \sum_{i=1}^{N_{days}}\sum_{j=1}^{N_{zones}} A_{i,j} \cap (SWE_{i,j} > \xi_{SWE}) \cap (\mathrm{SCA}_{i,j} = 0) \qquad (7)$$

where $A_{i,j}$ is the area of zone j on the day i which is cloud-free from MODIS. $SWE_{i,j}$ is the simulated snow water equivalent in elevation zone j larger than 10mm, $SCA_{i,j}$ is the snow covered area estimated from MODIS within this zone, N_{days} is the number of days i, where MODIS images are available with cloud cover less than a threshold (ξ_C) 50%.

The snow underestimation error indicates the relative number of days when the hydrologic model does not simulate snow in a zone, but MODIS indicates that snow covered area greater than a threshold 25% is present in the zone, i.e.:

$$S_U = \frac{1}{\sum_{i=1}^{N_{days}} \sum_{j=1}^{N_{zones}} A_{i,j}} \sum_{i=1}^{N_{days}} \sum_{j=1}^{N_{zones}} A_{i,j} \bigcap (SWE_{i,j} = 0) \bigcap (\mathrm{SCA}_{i,j} > \xi_{SCA}) \qquad (8)$$

The snow covered area, *SCA*, within each zone is calculated from the MODIS data as

$$\mathrm{SCA}=\mathrm{S}/(\mathrm{S}+\mathrm{L}) \qquad (9)$$

where S and L represent the number of pixels mapped as snow and snow free, respectively, for a given day and a given elevation zone.

The thresholds ξ_{SWE}, ξ_{SCA} and ξ_C are chosen on the basis of the sensitivity analysis performed by Parajka and Blöschl (2008). The procedure of model parameters calibration is carried out for each calibration variant and each catchment independently. All calibration variants are automatically calibrated by using the shuffled complex-self adaptive hybrid evolution (SC-SAHEL) developed by Naeini et al. (2018). It combines four evolutionary algorithms (EA) with the self-selected scheme and hence the evolution process of generating parameter values is more robust. The number of complexes is set to 8, allowing the four EAs to be automatically changed by each evolution generation. The optimization is stopped at any of the following three criteria: if the parameters converge to a space of geometric size less than 0.01; if the best objective function value has not improved by 0.1% over the last 10 loops; if the total number of runs reaches 1,000,000 (see. Chu et al., 2011; Naeini et al., 2018).

The calibration period used in all variants is from September 1, 2000 to August 31, 2010. The validation period is from September 1, 2010 to August 31, 2014. The warmup period is one year before the start of the calibration or validation period. Since soil moisture satellite data are available only from January 2007, the soil moisture simulation efficiency for the calibration period is calculated for a shorter time period.

4 Results

4.1 Performance of multiple objective calibration

The calibration model performance of three multiple objective calibration variants is presented in Figure 3 and Table ~~5~~4. The objective function involves a runoff component weighted by w_Q and additional soil moisture and snow components (Table ~~4~~3). The limiting case is w_Q=1 where only the runoff component is used and this case represents a typical calibration to runoff only. The case where w_Q=0 represents calibration only to SSM and/or SSC without the use of runoff data. The median runoff efficiency over the 213 catchments (Figure 3, top; Table ~~5~~4) ranges between 0.74 and 0.79 for w_Q larger than 0.3 irrespective of the calibration variants. Using SSM and SSC with runoff for model calibration results in a similar pattern of model performance to the case when only SSM and runoff are used, but the former variant has a smaller regional variability (scatter)

of runoff model efficiency for w_Q less than 0.6. Interestingly, when no runoff is involved (w_Q=0), using only SSC results in slightly better runoff simulations than when using only SSM, while for w_Q from 0.1 to 0.3 the opposite is the case.

The correlation between ASCAT and simulated soil moisture (Figure 3, centre) has a much larger regional variability (i.e. variability between catchments) than the w_Q variants. For the SSM and runoff variant, the median ~~of~~ correlation increases from 0.29 to 0.52 with decreasing w_Q, and the variant using all three variables is similar. For the snow cover and runoff variant w_Q has little effect on soil moisture correlation and correlation is similar to the runoff only calibration (w_Q=1).

Similar patterns are observed for the snow cover efficiency. The SSM weighting has little effect on the snow cover simulations. The median O_{SC} is between 0.75 and 0.79 for w_Q larger than 0.0. The variants that use SSC show increasing performance with decreasing w_Q and the regional variability decreases. For w_Q less than 0.5, the median O_{SC} is between 0.84 to 0.91, which is 5 to 13% larger than the median for calibration to runoff only (O_{SC} =0.79). These results indicate that the simultaneous use of SSM and SSC in model calibration can improve simulations of soil moisture and snow cover in the calibration period, without any significant reduction in runoff model efficiency, particularly for w_Q between 0.3 and 0.4.

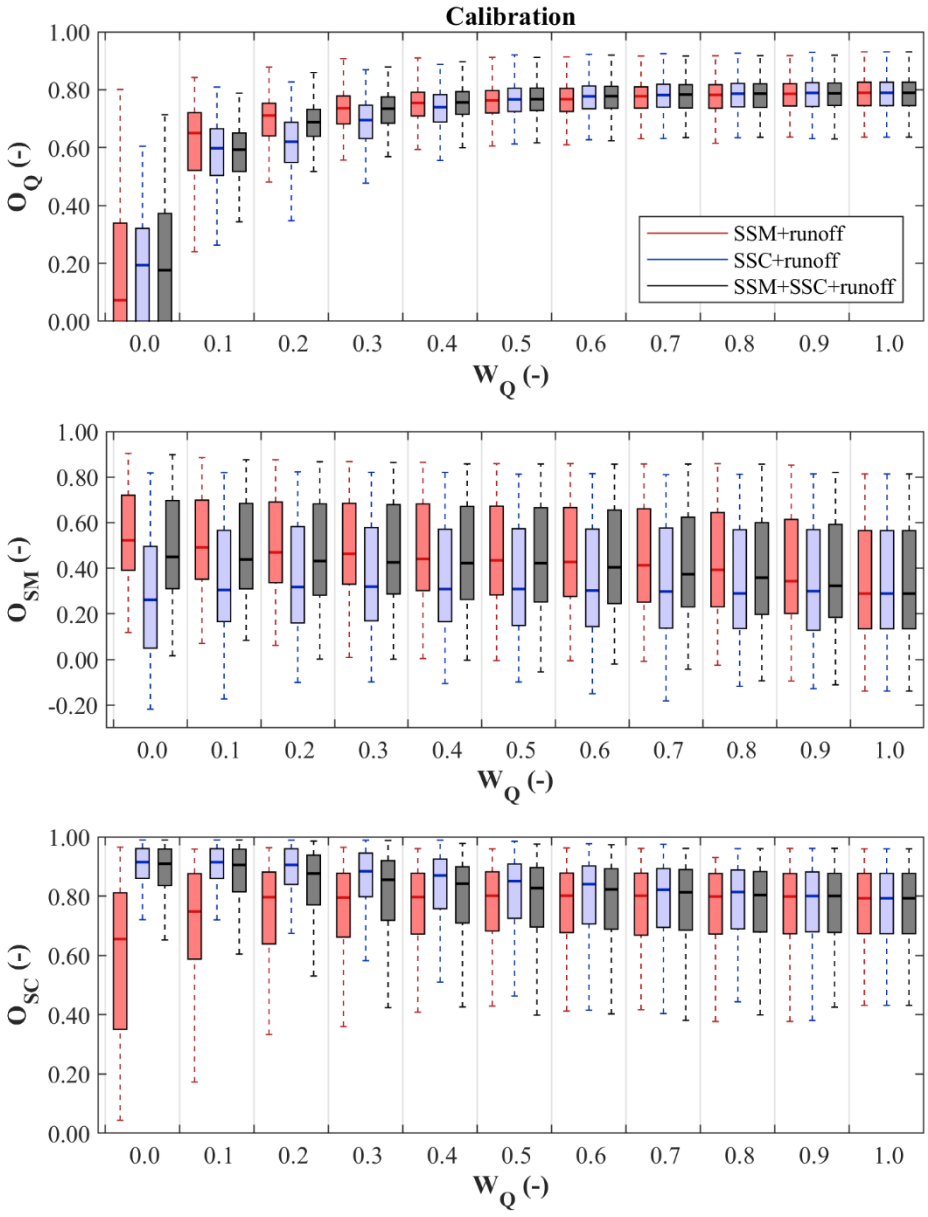
Calibration
1.00
0.80
0.60
0.40
0.20
0.00
O_Q (-)
SSM+runoff
SSC+runoff
SSM+SSC+runoff
0.0 0.1 0.2 0.3 0.4 0.5 0.6 0.7 0.8 0.9 1.0
W_Q (-)
1.00
0.80
0.60
0.40
0.20
0.00
-0.20
O_{SM} (-)
0.0 0.1 0.2 0.3 0.4 0.5 0.6 0.7 0.8 0.9 1.0
W_Q (-)
1.00
0.80
0.60
0.40
0.20
0.00
O_{SC} (-)
0.0 0.1 0.2 0.3 0.4 0.5 0.6 0.7 0.8 0.9 1.0
W_Q (-)

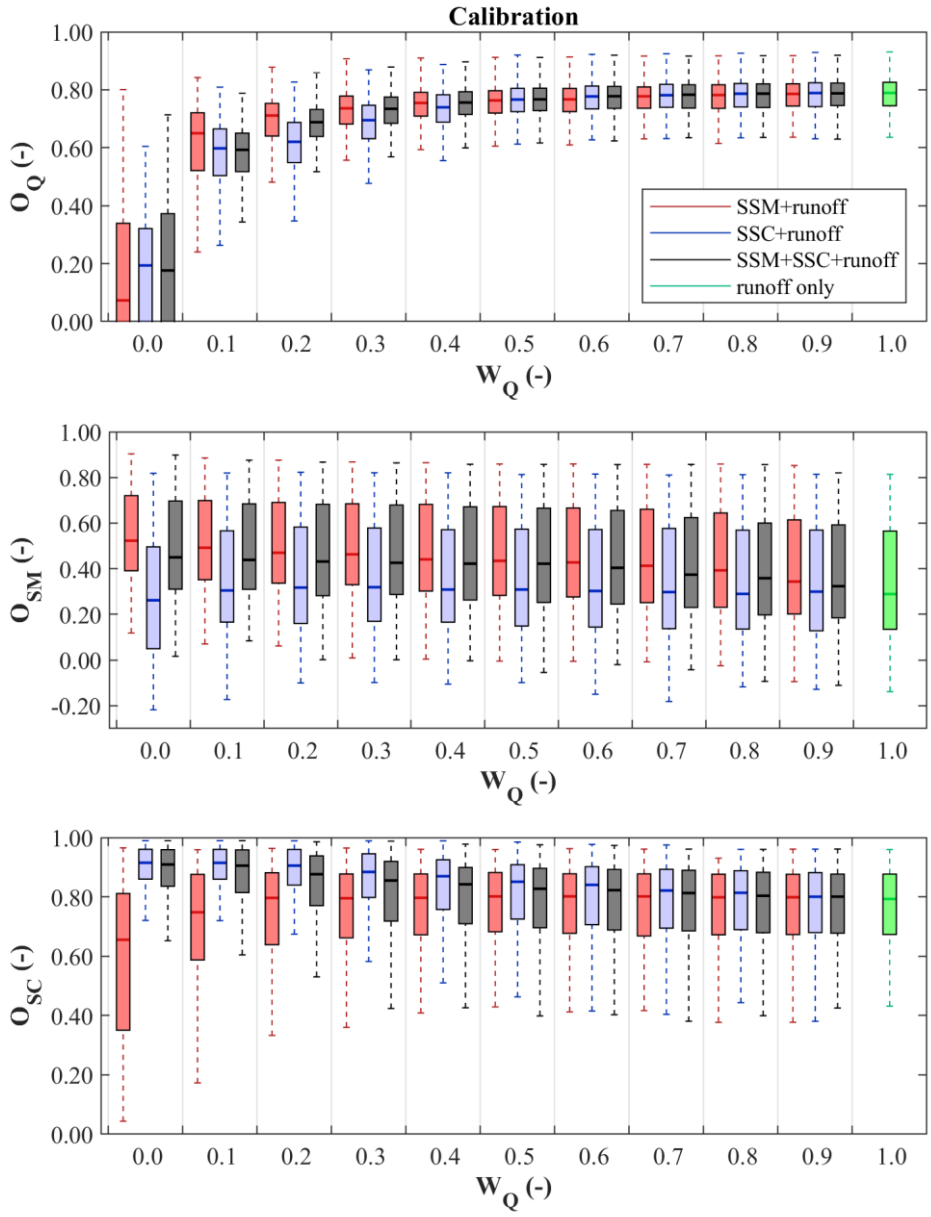

Figure 3: Hydrologic model performance for three multiple objective calibration variants: calibration to satellite soil moisture and runoff (red boxes), to satellite snow cover and runoff (blue boxes) and to satellite soil moisture, snow cover and runoff (grey boxes). Top, middle and bottom panels show runoff (Eq. 2), soil moisture (Eq. 5) and snow cover (Eq. 6) model efficiency for different weights of the runoff objective w_Q in the calibration period 2000-2010, respectively. w_Q =1 represents calibration to runoff only. ~~Size~~Boxes represent the values from the different catchments and the size of the boxes represents the spatial variability across the 213 catchments.

The model performance for the validation period (2010-2014) is presented in Figure 4 and Table ~~6~~5. The patterns of changing model efficiency with changing w_Q are very similar to those in the calibration period. The median of validation runoff model efficiency of the SSM and runoff calibration variant for w_Q >0.3 is between 0.71 and 0.73, which is similar or only somewhat smaller than that for calibration to runoff only (w_Q=1). The SSC and runoff calibration variant results show a slightly lower runoff model performance for weights w_Q< 0.3. The calibration with all three variables gives practically identical validation efficiencies as the variant with SSM and runoff.

The median soil moisture correlation increases from 0.43 to 0.54 with decreasing w_Q for the SSM and runoff calibration variant and ranges from 0.42 to 0.49 for the variant that uses all variables. The smallest correlations are found for the SSC and runoff variant, where the median of correlation *r* varies between 0.35 and 0.43. The regional variability in *r* is however much larger for all variants than for the calibration period. The scatter (i.e. difference between 75- and 25- percentiles) in *r* is around 0.3 for all w_Q. For the variants that include SSM the 75-percentiles vary between 0.60 and 0.68.

The snow cover efficiency for w_Q larger than 0.5 is very similar for all three variants. For w_Q smaller than 0.5, O_{SC} tends to increase and the regional variability decreases for the variants involving SSC. The validation O_{SC} is about 2% larger than that obtained in the calibration period. Similar to the calibration period, the weighting of SSM and runoff has hardly any impact on O_{SC}. Adding SSC data to SSM and runoff improves the snow simulation, particularly for w_Q less than 0.4.

It is also interesting to compare the relative performances in the validation period to that in the calibration period.

The runoff model performance always decreases when moving from the calibration to the validation period, although the decrease is relatively small, suggesting that there is no overfitting. The soil moisture model performance in contrast always increases when moving from the calibration to the validation period. This is likely because in the case of soil moisture the calibration period only consists of about four years. The snow model performance increases slightly, probably because the proportion of day with temperatures below 0 °C for the validation period is 0.21, which is lower than that for the calibration period (0.24), but the precipitation during the days with the air temperature below 0 °C does not show obvious changes (2.62 mm·day^{-1} for the calibration and 2.67 mm·day^{-1} for the validation periods).

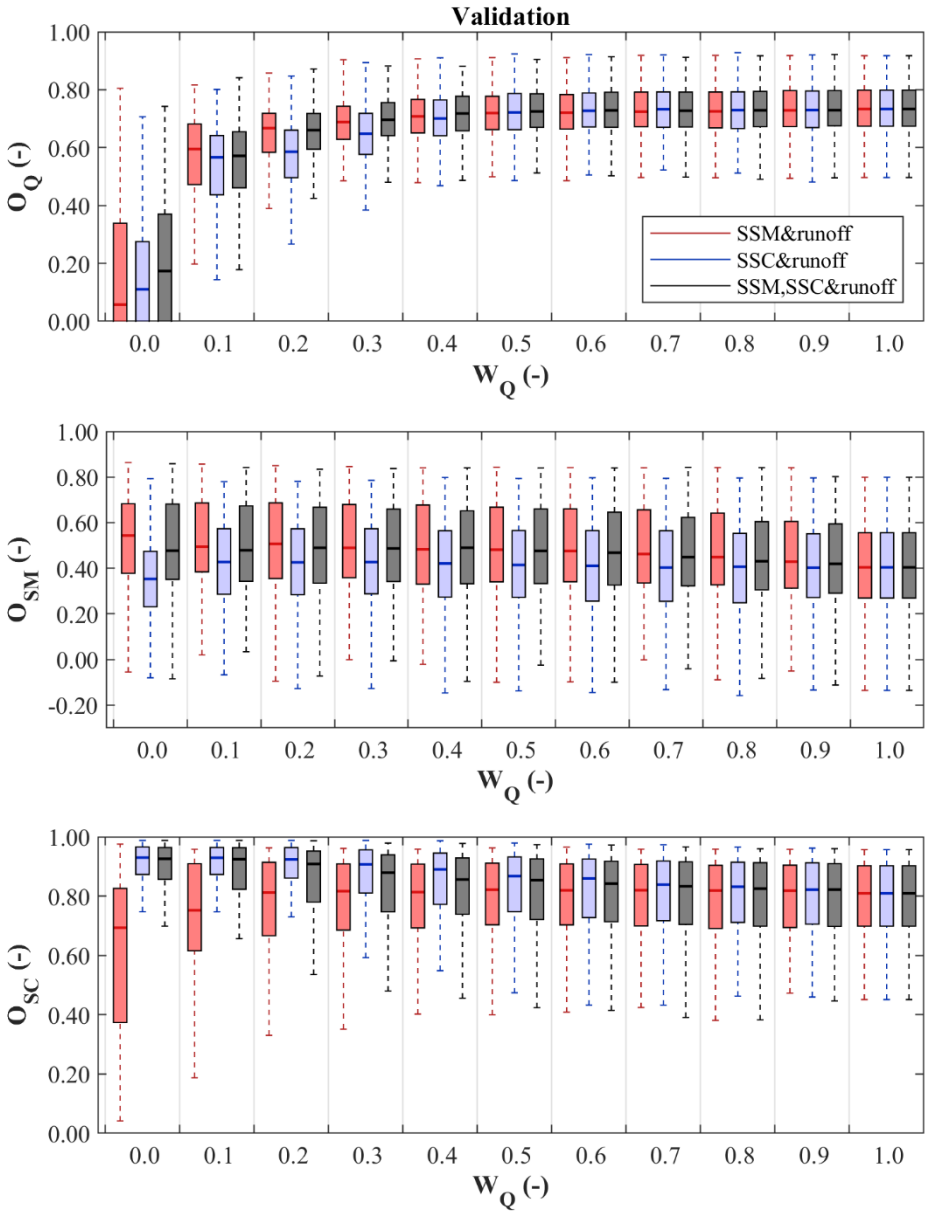
Validation
1.00
0.80
0.60
0.40
0.20
0.00
O_Q (-)
SSM&runoff
SSC&runoff
SSM,SSC&runoff
0.0 0.1 0.2 0.3 0.4 0.5 0.6 0.7 0.8 0.9 1.0
W_Q (-)
1.00
0.80
0.60
0.40
0.20
0.00
-0.20
O_{SM} (-)
0.0 0.1 0.2 0.3 0.4 0.5 0.6 0.7 0.8 0.9 1.0
W_Q (-)
1.00
0.80
0.60
0.40
0.20
0.00
O_{SC} (-)
0.0 0.1 0.2 0.3 0.4 0.5 0.6 0.7 0.8 0.9 1.0
W_Q (-)

280

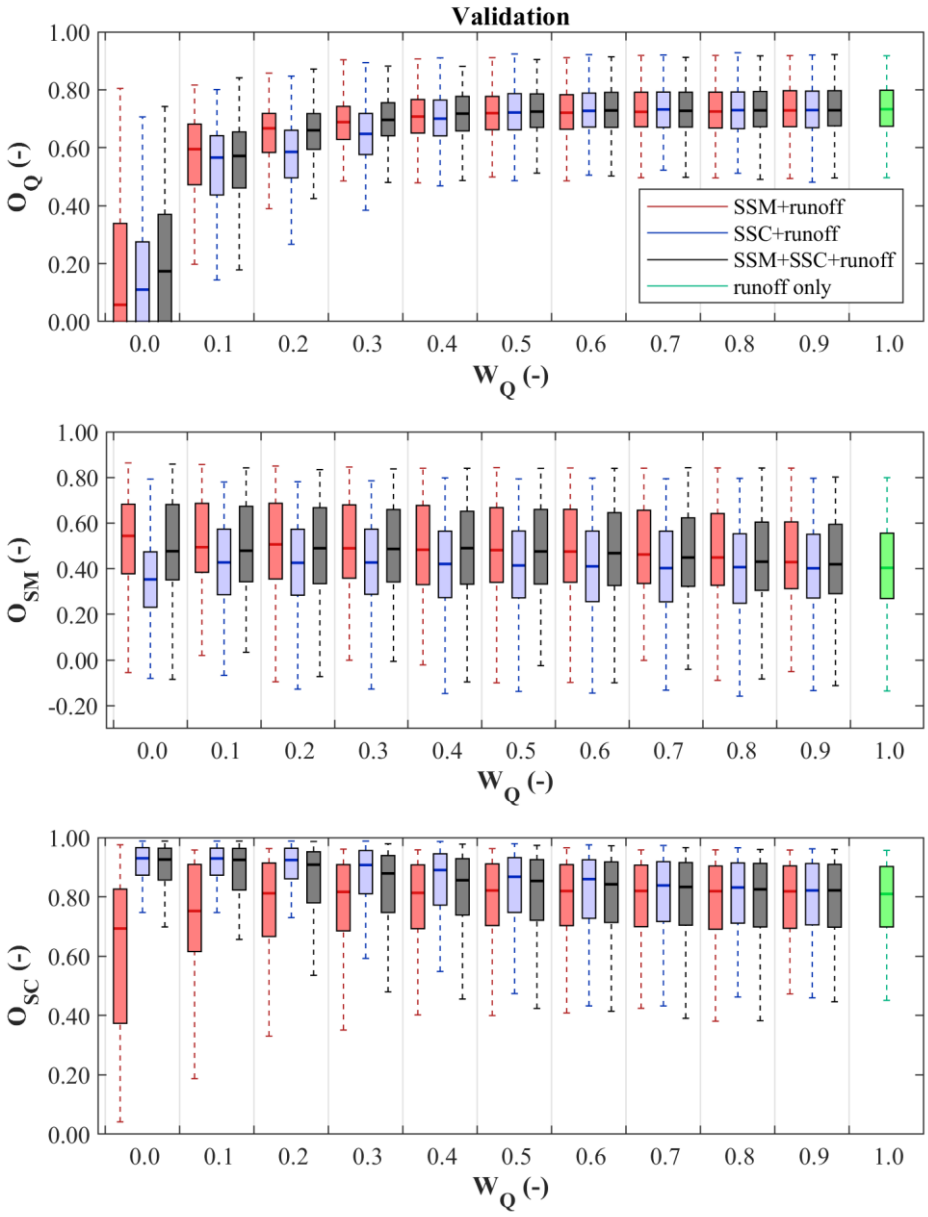

Figure 4: Hydrologic model performance for three multiple objective calibration variants: calibration to satellite soil moisture and runoff (red boxes), to satellite snow cover and runoff (blue boxes) and to satellite soil moisture, snow cover and runoff (grey boxes). Top, middle and bottom panels show runoff (Eq. 2), soil moisture (Eq. 5) and snow cover (Eq. 6) model efficiency for different weights of the runoff objective in the validation period 2010-2014, respectively. w_Q =1 represents calibration to runoff only. ~~Size~~Boxes represent the values from the different catchments and the size of the boxes represents the spatial variability across the 213 catchments.

The correlation (in terms of the Pearson correlation coefficient) between model performance and selected catchment attributes (Table ~~2~~1) is evaluated in Figures 5 and 6 in order to understand in which type of catchments SSM and SSC have the most relevant effect on model performance. The runoff model efficiency during the calibration period (Figure 5, left panel) increases with the increasing mean number of days with negative air temperatures (MTL0, correlation over 0.57 for w_Q larger than 0.4) and mean catchment elevation (MELE, correlation over 0.55 for w_Q larger than 0.4) and tends to decrease with increasing catchment mean annual air temperature (MAT, absolute correlation over 0.57 for w_Q larger than 0.4). The larger runoff model efficiency in Alpine catchment than in the lowlands is likely related to the seasonality of snowmelt runoff which is easier to simulate than the individual, more erratic events in the lowlands (Merz and Blöschl, 2009). The correlation of runoff model efficiency and catchment attributes increases with increasing runoff weight w_Q and is not statistically significant or low (i.e. less 0.4) for w_Q<0.4 for most of the attributes. The correlations of the catchment attributes with soil moisture and snow efficiencies are not consistently related to runoff weight. Soil moisture efficiency increases with increasing fraction of agricultural land (AP) where the correlation varies between 0.75 and 0.79 for different w_Q. This trend may be explained by the fact that soil moisture can generally be monitored more accurately in relatively flat, agricultural landscape than in rugged mountainous terrain (Brocca et al. 2013; Parajka et al., 2006), which in Austria are furthermore dominantly covered by forests and other dense vegetation impenetrable to the radar and scatterometer signals~~–~~. Accordingly, we find the~~–~~ soil moisture efficiency tends to decrease with increasing forest cover (FP, correlation varies between -0.35 and -0.49). The active rooting zones are much shallower in agricultural lands, whereas trees root much deeper. Hence the satellite soil moisture data used in this study which monitored for the top 100 cm soil layer may fit the soil moisture for arable land better. Also snow model efficiency tends to increase with decreasing MELE and SL (correlation is between -0.52 to -0.89), but increases with increasing MAT (correlations exceed 0.8 for most of the w_Q). In the flatlands, snow is less important so the cumulative number of days with potential snow errors in the objective function is generally lower.

The correlations for the validation period (Figure 6) have the same pattern as for the calibration period (Fig.5). The attributes with the largest correlations with runoff efficiency are the same and correlation tends to increase with increasing w_Q as well. The correlation is generally only slightly lower than that estimated in the calibration period. The soil moisture efficiency in the validation period is positively correlated with AP (correlation = 0.76-0.79) and MAT (correlation = 0.55-0.68), but the correlation with AP is lower than in the calibration period. The largest negative correlation of soil moisture efficiency and attributions is found for calibration to runoff only (w_Q=1) in general and is larger than 0.7 for ~~SL, FP~~MELE, catchment elevation range (ER), and standard deviation of MAT and mean daily potential global radiation (SDGR). The snow model efficiency is clearly related to topography, as it increases with decreasing MELE and increasing MAT.

The relationship between model efficiencies and catchment attributes for the other two calibration variants are similar and are presented in Supplement, Figs ~~S1-S4~~S3-S6. The results show that including snow or soil moisture data in model calibration does not change the correlation between model efficiencies and catchment characteristics. It is obvious that for runoff weight

w_Q>=0.4 for O_Q, w_Q>=0.0 for O_{SM}, and w_Q>=0.1 for O_{SC}, the correlations between model efficiency and catchment characteristics are similar to that for the runoff only calibration. The model efficiency is mainly related to topography and certain climate, land cover and soil attributes, which are, on the other hand, cross-correlated with topography (Figure ~~S1~~S3).

325

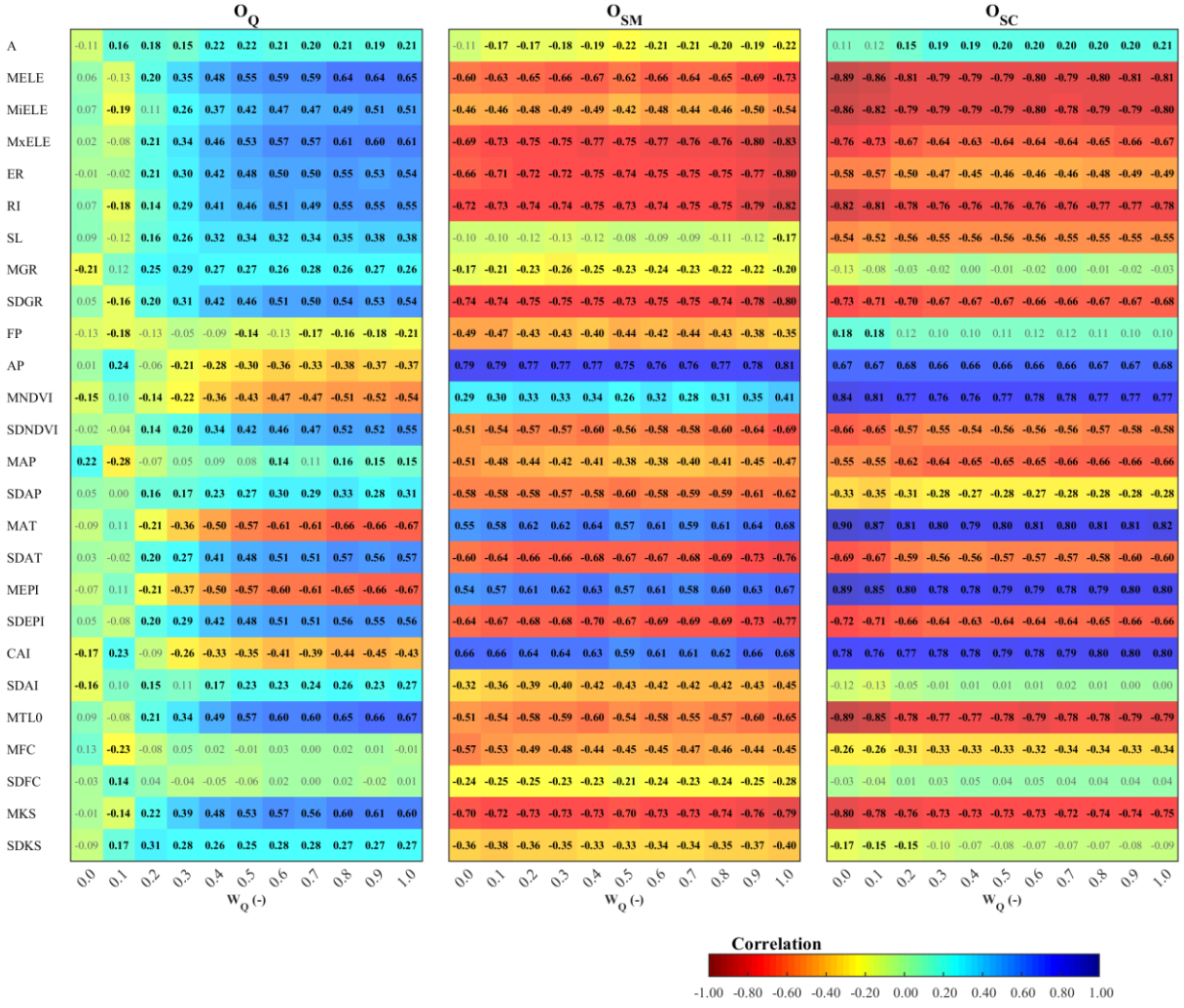

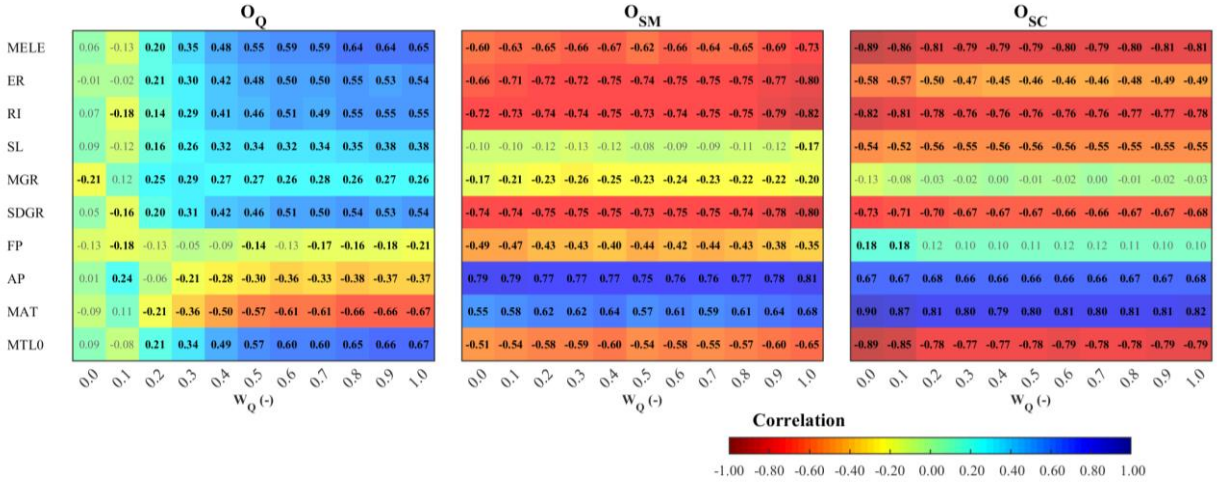

Figure 5: Correlation between catchment attributes (Table ~~2~~1, other attributes can be found in supplementary Figure S1) and model performance, i.e. runoff (Eq. 2, left panel), soil moisture (Eq. 5, middle panel) and snow cover (Eq. 6, right panel), obtained from multiple objective calibration to satellite soil moisture (ASCAT), satellite snow cover (MODIS) and runoff (Var 3 of Table 4, SSM+SCM+runoff) in the calibration period 2000-2010. Cool and warm colors represent positive and negative correlations, respectively. Bold print indicates significance with p-value lower than 0.05.

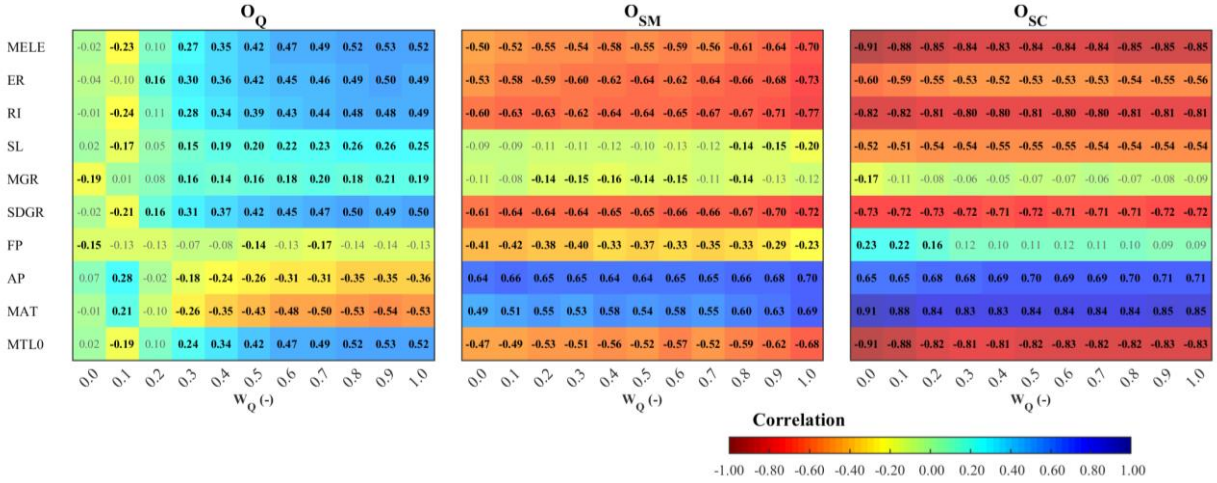

Figure 6: Correlation between catchment attributes (Table 1, other attributes can be found in supplementary Figure S2) and model performance, i.e. runoff (Eq. 2, left panel), soil moisture (Eq. 5, middle panel) and snow cover (Eq. 6, right panel), obtained from multiple objective calibration to satellite soil moisture (ASCAT), satellite snow cover (MODIS) and runoff (Var 3 of Table 5, SSM+SCM+runoff) in the ~~calibration~~validation period ~~2000~~ 2010-2014. Cool and warm colors represent positive and negative correlations, respectively. Bold print indicates significance with p-value lower than 0.05.

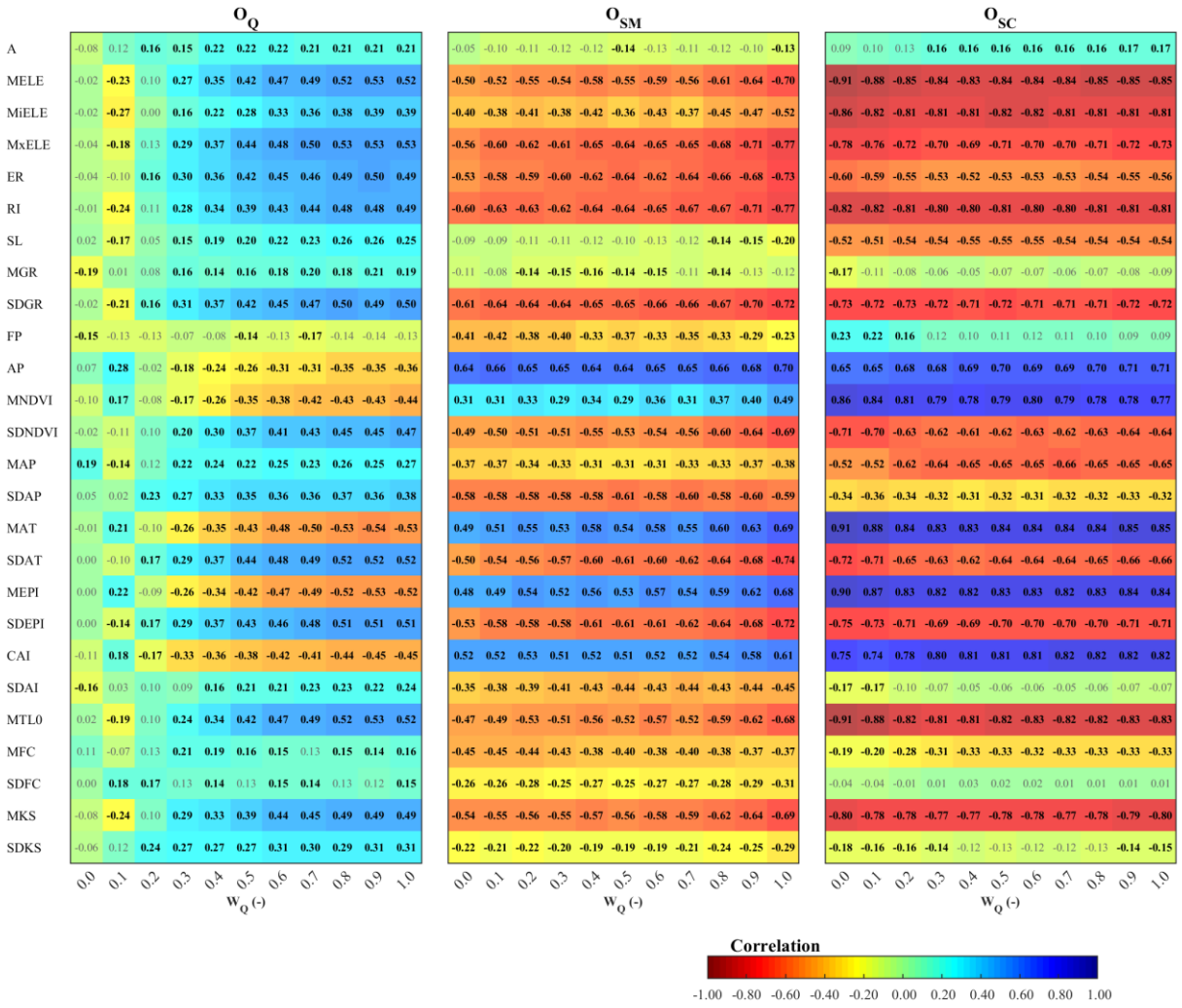

~~**Figure 6: Correlation between catchment attributes (Table 2) and model performance, i.e. runoff (Eq. 2, left panel), soil moisture (Eq. 5, middle panel) and snow cover (Eq. 6, right panel), obtained from multiple objective calibration to satellite soil moisture (ASCAT), satellite snow cover (MODIS) and runoff (Var 3 of Table 6) in the validation period 2010-2014. Cool and warm colors represent positive and negative correlations, respectively. Bold print indicates significance with p-value lower than 0.05.**~~

4.2 Variability in calibrated model parameter values

Figure 7 compares the medians of the model parameters for all catchments obtained with the three multiple calibration variants, grouped by snow, soil, runoff generation and runoff routing parameters in the columns from left to right. The snow-related parameters (left column) are similar for the two calibration variants that use satellite snow cover~~, while~~. In contrast the variant that uses soil moisture and runoff tends to have different values, particularly for the threshold temperature parameters (Tr, Ts, Tm). The medians of the snow correction (SCF) and melt (DDF) factors tend to be similar in all three variants if $w_Q > 0.4$.

The soil-related parameters (2nd column) show similar patterns. The variants that use satellite soil moisture in model calibration have more similar soil model parameter values than the one that uses only SSC and runoff. This suggests that adding soil moisture satellite data in model calibration affects the soil-related parameters strongly and adding snow and soil moisture satellite data is complementary for influencing both snow and soil moisture related parameters. The similarity of the variant using all three variables with those variants where alternatively SSC and SSM are left out suggests that SSC is more important for the snow-related parameters, and SSM is more important for the soil-related parameters, as would be expected. Increasing the runoff weight tends to decrease the difference between the calibration variants of the snow-related and the soil-related parameters. The runoff generation-related parameters (3rd column) tend to be more similar for the two variants that use SSC, and the runoff routing-related parameters (right column) are always rather similar.

In ~~a~~the next step the model parameters obtained by multiple objective calibration are compared with those obtained by traditional calibration to runoff only (~~Fig.~~Figure 8). The figure shows that the similarity between model parameters decreases with decreasing w_Q.

Snow-related parameters calibrated using SSC (middle column, top five lines) deviate quickly from those using runoff only as w_Q decreases. Similarly, the soil-related parameters calibrated using SSM (left column, lines 6-8 from top) deviate quickly from their counterparts based only on runoff calibration. The difference in similarity/correlation between multiple objective calibration variants and runoff only calibration is smaller for runoff generation parameters. The runoff routing model parameters seem to be not very sensitive to selected model efficiencies and the correlation between model parameters is very small.

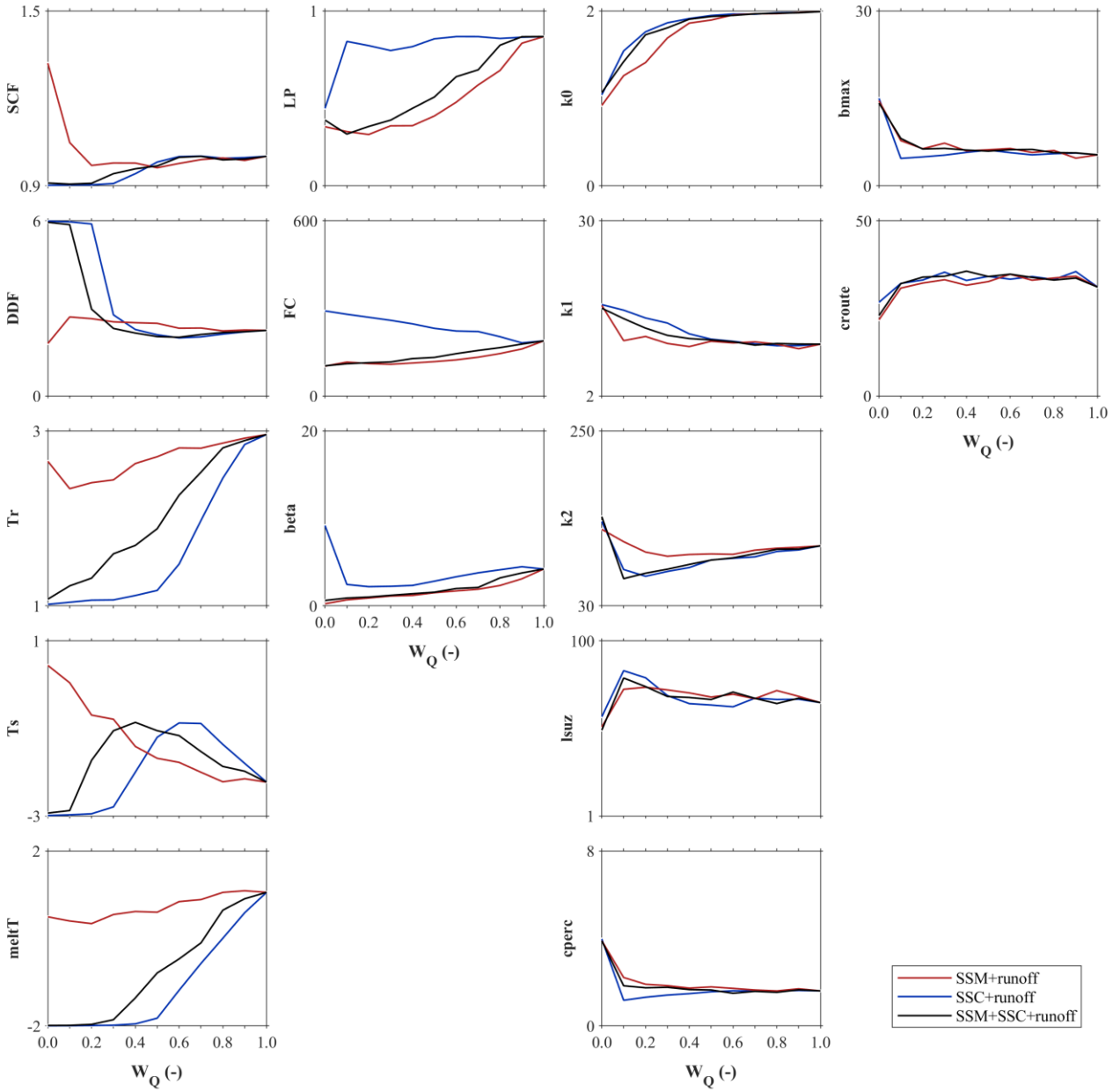
SCF
LP
k0
bmax
DDF
FC
k1
croute
Tr
beta
k2
Ts
lsuz
meltT
cperc
W_Q (-)
SSM+runoff
SSC+runoff
SSM+SSC+runoff

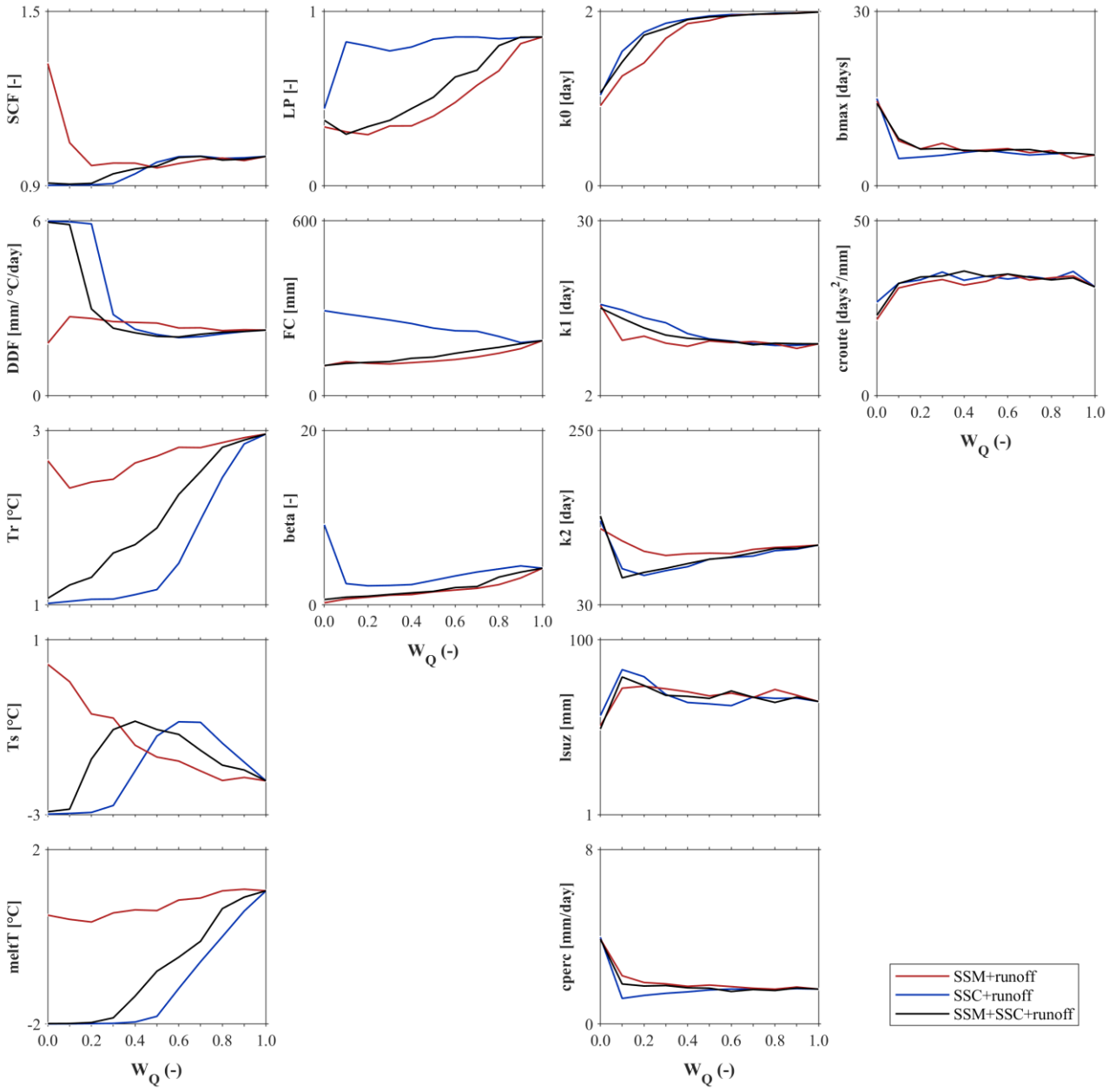

Figure 7: Medians of the parameter values from the three multiple objective calibration variants (lines) and different runoff weights w_Q (Table 43). Red, blue and grey lines represent the calibration variants using soil moisture and runoff, snow cover and runoff, and soil moisture, snow cover data and runoff, respectively. Lines represent the median of the 213 Austrian catchments.

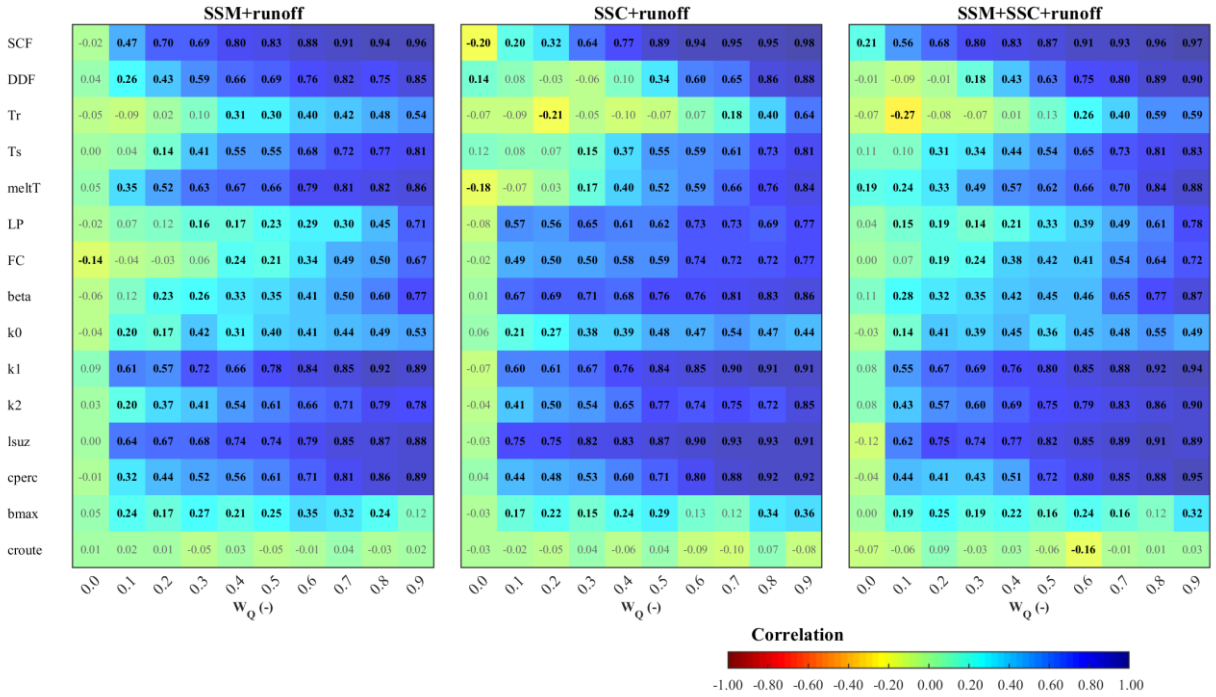
SSM+runoff
SSC+runoff
SSM+SSC+runoff
SCF
DDF
Tr
Ts
meltT
LP
FC
beta
k0
k1
k2
lsuz
cperc
bmax
croute
0.0 0.1 0.2 0.3 0.4 0.5 0.6 0.7 0.8 0.9
W_Q (-)
Correlation
-1.00 -0.80 -0.60 -0.40 -0.20 0.00 0.20 0.40 0.60 0.80 1.00

385

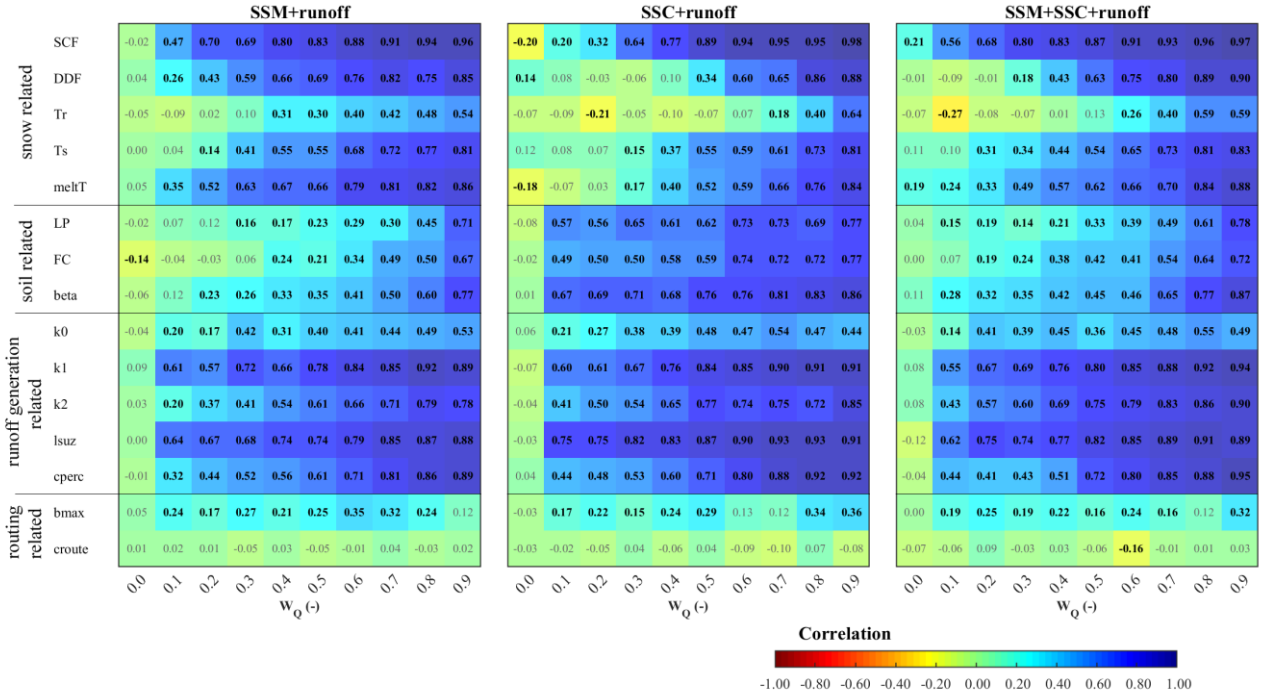

Figure 8: Correlation of parameter values from three multiple objective calibration variants (runoff weights w_Q = 0.0 to 0.9, Table ~~4~~3) with those from traditional calibration to runoff only (w_Q=1.0). Left, middle and right panels represent calibration variants using soil moisture and runoff, snow cover and runoff and all three variables, respectively (Var 1, 2, 3 of Table ~~5~~4 and ~~6~~5). Cool and warm colors represent positive and negative correlations, respectively. Bold print indicates significance with p-value lower than 0.05.

4.3 Comparison of multiple objective and runoff only calibration ~~to calibration to runoff only~~efficiencies

The relative difference between the model efficiency of the three multi-objective variants and that based on calibration to runoff only is presented in Figure 9. The runoff model efficiency of multiple objective calibration tends to be slightly lower than the traditional calibration to runoff only. The median of difference in runoff model efficiency of the two variants that ~~uses~~use SSM in model calibration is less than 3.2% for w_Q larger than 0.3 in both calibration and validation periods. The multiple objective calibration to SSC- and runoff has a somewhat larger median of difference for w_Q between 0.2 and 0.4, but for larger w_Q the median is almost identical with that of the other multiple objective variants. The integration of soil moisture in model calibration improves the correlation of satellite and simulated soil moisture. The median improvement for w_Q <0.6 is larger than 30% and 15% in the calibration and validation periods, respectively. The calibration to all variables has a median relative improvement about ~~4~~3% to ~~25~~35% lower than the calibration to SSM and runoff in the calibration period, but is very

similar in the validation period. The calibration to SSM and runoff does not improve snow cover simulations, but the use of all variables improves the snow model efficiency. For w_Q less than 0.5 the median improvement is larger than 5% in both calibration and validation periods.

Given that the median runoff efficiency is not improved by the addition of soil moisture and snow data (Figure 9) it is of interest to see how the changes are distributed in space. Figure 10 shows that in up to 40% of catchments the validation runoff efficiency is improved by using multiple objective calibration as compared to calibration to runoff alone. The number of catchments with runoff improvements increases with increasing runoff weight. The flipside, of course, is that in the remaining catchments the runoff model efficiency ~~is deteriorated~~deteriorates. The calibration variants that use SSM data improve soil moisture simulations in more than 80% of the catchments for all weights, and the addition of snow data does not change the performance. The snow model efficiency is vastly improved by the inclusion of the SSC data, for w_Q ~~>~~≤0.6 in almost all catchments, and the inclusion of soil moisture (in the variant that uses all variables) has still a very big improvement of snow simulations as compared to the case when only runoff is used in the calibration.

Overall, there are two important messages. The inclusion of soil moisture data in the calibration mainly improves the soil moisture simulations; the inclusion of snow data in the calibration mainly improves the snow simulations; and including both of them improves both soil moisture and snow simulations to a similar extent. Second, when comparing the panels of Figure 10, one sees that the snow data are more efficient in improving snow simulations than the soil moisture data are in improving soil moisture simulations.

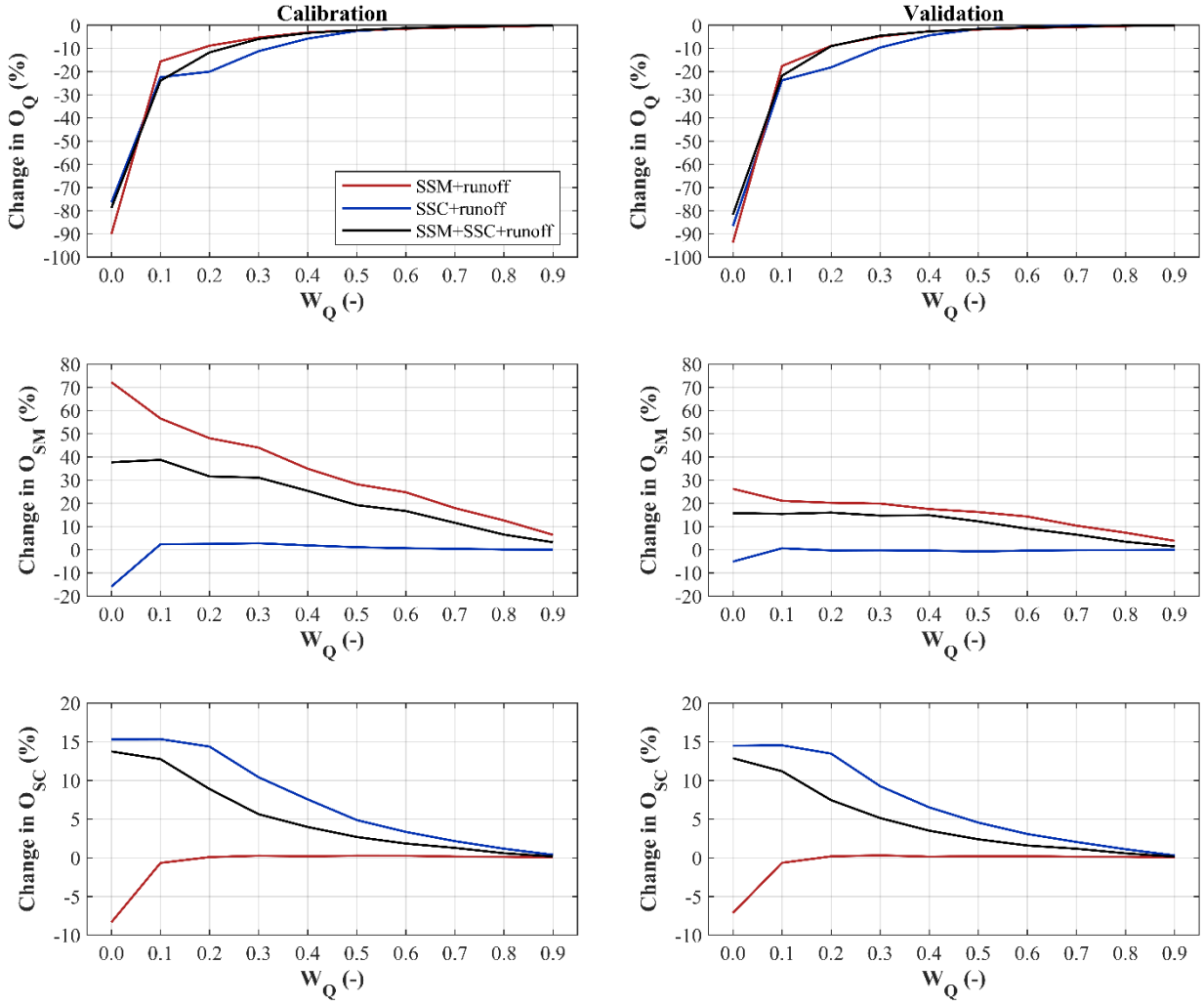

Figure 9: Relative difference in model efficiency of three multiple objective calibration variants (lines) using different runoff weights w_Q (Table 43) compared to traditional calibration to runoff only (w_Q=1). Red, blue and grey lines represent calibration variants using soil moisture and runoff, snow cover and runoff, and soil moisture, snow cover and runoff, respectively Lines represent the median of the 213 Austrian catchments. Top, middle and bottom panels refer to runoff, soil moisture and snow cover efficiencies in the calibration (left panels) and validation (right panels) periods, respectively.

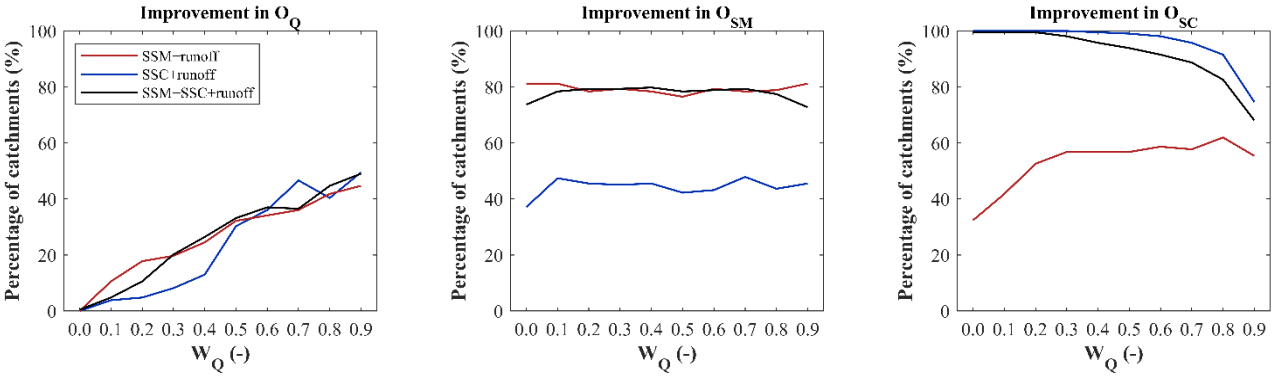

Figure 10. Relative number of catchments with improvement in runoff (left), soil moisture (centre) and snow cover (right) model efficiency in the validation period. Relative number relates to the 213 Austrian catchments used in this study.

It is now of interest to see whether the catchments for which the runoff and soil moisture model efficiencies are improved by the inclusion of SSC and SSM data (Figure 10) are different from those for which this is not the case. The distribution of the catchment attributes of these two catchment groups are therefore compared with the Kolmogorov-Smirnov two sample test (KS). Since the snow model efficiency is improved in almost all study catchments, it is not analysed here. Table ~~7~~S2 and Table ~~8~~S3 show the p–values of the KS for the runoff and soil moisture model efficiencies, respectively, indicating statistically significant differences between the catchment groups in many cases. For catchments with a large frequency of runoff improvements (e.g. for w_Q = 0.7 and 0.8) there are a number of differentiating factors including those related to topography (mean catchment elevation, mean catchment slope), proportion of agricultural land, mean annual air temperature, number of days with negative air temperature and mean saturated hydraulic conductivity. An example of differences between the groups in terms of mean catchment elevation (MELE) and percentage of arable land (AP) is presented in Fig. 11. The results indicate that improvement in runoff is observed in catchments with lower mean catchment elevation and a larger proportion of agricultural land. The other catchment attributes with statistically significant differences are correlated with MELE, so have similar differences in the distributions as those presented in ~~Fig. 11~~Figure S7.

Since an improvement in soil moisture simulations is observed in 80% of the catchments (Fig. 10) their attributes are particularly interesting. The factors controlling the improvement include topographical (MELE, SL, ER, SDGR), land cover (FP, AP), climate (MAP, SDAP, MAT, CAI, MTLT0) and soil (MKS) attributes, similarly as for improvement in runoff. This is illustrated in ~~Fig. 12~~Figure S8 that indicates that improvement in soil moisture simulations occurs particularly in catchments with low mean catchment elevation and a large proportion of agricultural land. In contrast to the runoff improvements, the results for the improvement in soil moisture are not related to the runoff weight w_Q used in the model calibration.

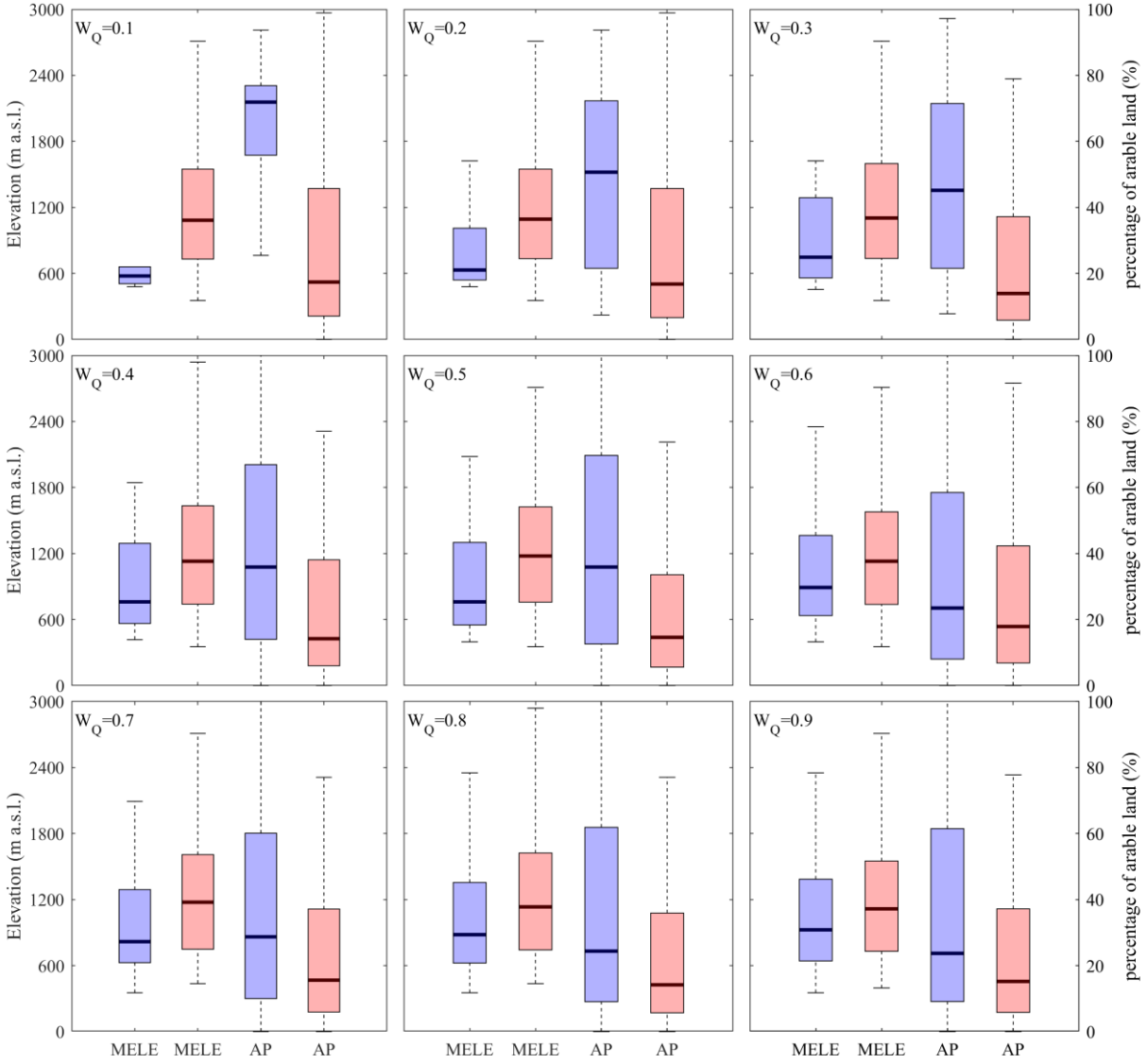

455

~~Figure 11: Distributions of mean catchment elevation (MELE) and percentage of arable land (AP) for the groups of catchments with (blue) and without (red) runoff model efficiency improvement in the validation period when including soil moisture and snow data in the calibration.~~

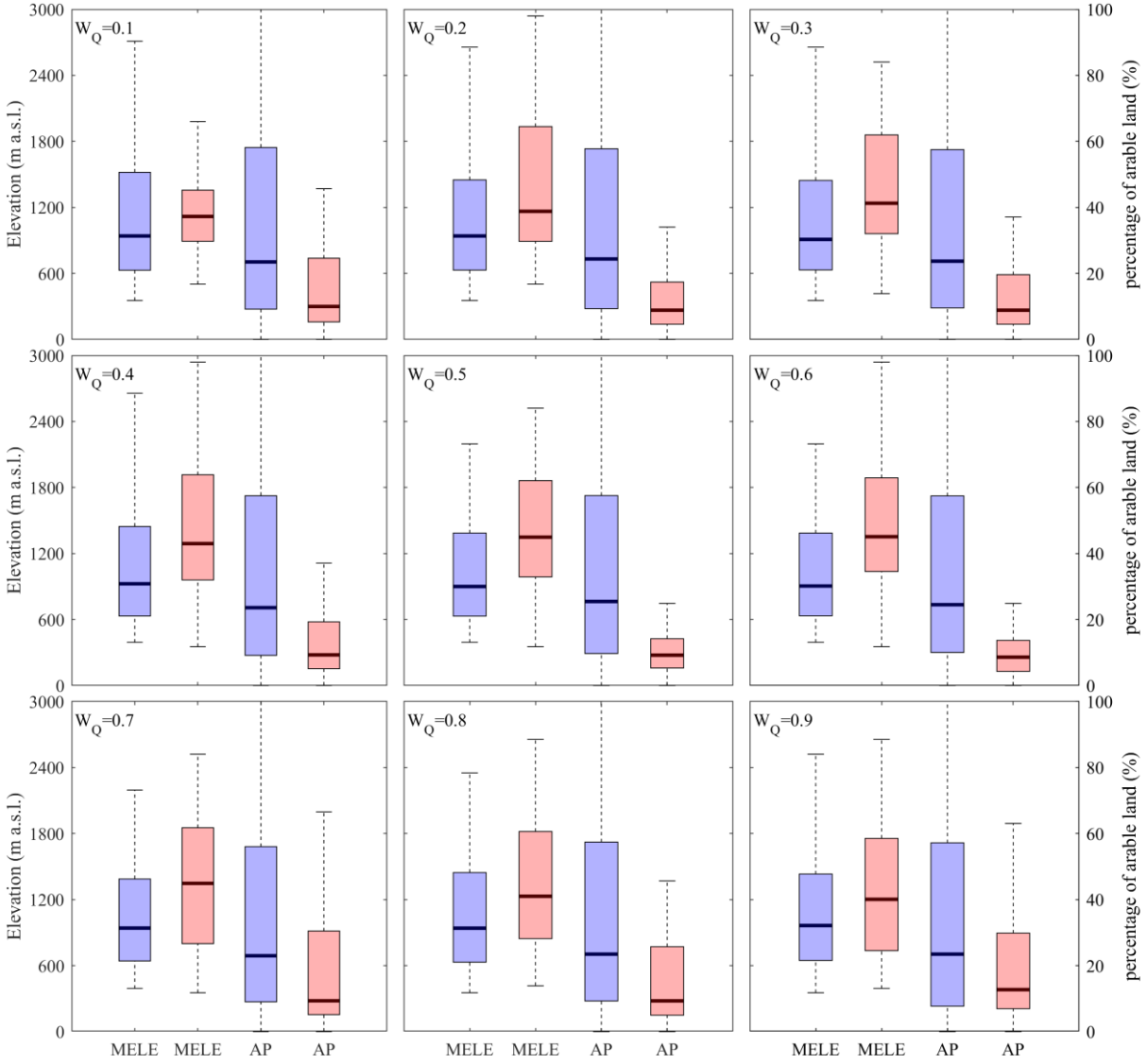

460 **~~Figure 12: Distributions of mean catchment elevation (MELE) and percentage of arable land (AP) for the groups of catchments with (blue) and without (red) soil moisture model efficiency improvement in the validation period when including soil moisture and snow data in the calibration~~**

5 Discussion and conclusions

In this study, we tested three multiple calibration variants using runoff data along with ASCAT SWI soil moisture and MODIS snow cover data. The calibration runoff model efficiency is similar to previous studies (Parajka et al., 2008, 2009; Sleziak et al., 2018) that used only runoff for model calibration. For example, the median of runoff model efficiency ranges between 0.77-0.79 (for runoff weights larger than 0.4) which is similar to the medians of 0.80 and 0.84 found in Parajka et al. (2008, 2009) for 148 Austrian catchments, and better than the median of 0.76 found for 320 Austrian catchments in Parajka et al., (2006) as well as the range 0.70-0.73 found for the same set of catchments as in this paper but using a lumped model (Sleziak et al., 2018).

Results show that the inclusion of satellite soil moisture data in the calibration mainly improves the soil moisture simulations. The median soil moisture correlation between hydrologic model outputs and ASCAT SWI is 0.4 to 0.52 (depending on the weight w_Q), which is significantly larger than the median of 0.26 found by using the coarser ERS scatterometer data in model calibration in Parajka et al. (2006). This reflects improvements both in the instrument specifications (better temporal and spatial sampling, higher radiometric accuracy, etc.) and the retrieval algorithm (Naeimi et al. 2009, Hahn et al. 2020). The ASCAT product used in this research is the same product which is used as the active product in the ESA-CCI. The study of Dorigo et al. (2017) demonstrated the quality of the active ESA-CCI product over temperate climates such as Austria. Considering that the spatial sampling of the ESA-CCI dataset is 0.25 degree, whereas the ASCAT product has a sampling of 12.5 km, the ASCAT product was chosen to be applied in this study. In addition, the algorithm of the ASCAT product which improved vegetation parameters performed better over Austria (Pfeil et al., 2018).

The inclusion of satellite snow data mainly improves the snow simulations. Using MODIS snow cover data to constrain the model parameters shows strong ability in improving the accuracy of representing the snow accumulating and melting processes from the model. When giving weights w_Q<0.5 to snow, almost all the catchments showed improvements in snow cover simulations. In terms of the improvement in snow model efficiency, our results are better than the results from Parajka et al. (2008), in their study only 3 years MODIS snow cover data was used, the improvement of snow mapping even depended on the data availability.

The satellite snow data are more efficient in improving snow simulations than the satellite soil moisture data are in improving soil moisture simulations. Part of the reason may be related to problems in mapping soil moisture in the alpine region while MODIS snow cover is very accurate both in the lowlands and in the mountains. For example, Parajka and Blöschl (2006) and Tong et al. (~~2019~~2020) showed the classification accuracy of the MODIS snow cover range from 95% to over 97% in Austria. Furthermore, it is interesting that including both soil moisture and snow cover data improves both soil moisture and snow simulations to almost the same extent as if including them individually, without any significant deterioration in the other variable. This gives the possibility to consistently improve the simulations of snow and soil moisture in future model applications. Our validation results indicate that snow simulations are improved in almost all, soil moisture correlation in about

80% and runoff in up to 40% of the catchments. Overall, the runoff performance changes very little when including soil moisture and snow data in the calibration.

The calibrated snow-related parameters are strongly affected by including snow data, and to a lesser extent by soil moisture data, while the soil-related parameters are only affected by soil moisture data. This separation is a welcome property as it facilitates parameter calibration. The soil moisture data also have some effect on the snow-related parameters~~.~~, this is in consistence with Nijzink et al (2018). As the melting changes the soil moisture directly, the soil moisture data provide additional constraints on the parameters controlling snowmelt. This can be helpful in understanding hydrological processes, especially for the variation of snow water equivalent.

Our results indicate that the runoff and soil moisture simulation improvement when including soil moisture data in the calibration is found mainly in catchments with lower mean catchment elevation and a larger proportion of agricultural land. While, overall, in 40% of the catchments the validation runoff efficiency is improved by the inclusion of soil moisture (Figure 10, left panel), these are about 50% of the catchments if only those with elevation lower than the median (1011 m a.s.l) and agricultural area larger than its median (16.3%) are considered. Similarly, while, overall, in 80% of the catchments the validation soil moisture efficiency is improved by the inclusion of soil moisture (Figure 10, middle panel), these are about 90% of the catchments if only those which low elevation and agricultural use are considered. The higher efficiency in improving the hydrologic model in the lowlands can be explained by the better quality of the ASCAT soil moisture retrievals (compared to the alpine regions), but is likely also ~~-~~due to the higher spatial consistency in soil texture and land cover type, and also lower slope and elevation variation. In contrast to a previous assessment of ERS assimilation into model calibration (Parajka et al., 2006), we found soil moisture improvement not only in lowland catchments with lower topographical variability, but also in catchments with smaller sizes (Figure 5) which may be related to the higher spatial and temporal resolution of ASCAT as compared to ERS. Over flatlands, ASCAT retrievals have improved a lot compared to the ERS retrievals 15 years back, but in alpine regions, the rugged topography, dense alpine vegetation, and presence of snow and ice even during the summer, makes using the data still challenging, given the higher retrieval errors and invalid measurements when the ground is snow covered or frozen. Additionally, the large heterogeneity in temperature and snow cover in mountainous regions can lead to insufficient masking for frozen soil and snow cover.

This study has evaluated the potential of assimilating the soil water index (representing root zone soil moisture) into hydrologic model calibration. It would be useful to extend this study to assimilate other variables, such as surface soil moisture estimates by using a dual soil moisture conceptual hydrologic model (Parajka et al., 2009) and also compare the role of the spatial resolution of soil moisture and snow data on their value in the assimilation.

Data availability

The discharge data from the HZB can be accessed through https://ehyd.gv.at/ (BMLRT, 2020). The meteorological data from the ZAMG are currently not freely available, requests should be directed to klima@zamg.ac.at. The ASCAT soil moisture data is available via Copernicus Global Land Service (https://land.copernicus.eu/). MODIS C6 snow cover products are from NASA

National Snow & Ice Data Center (https://nsidc.org/). Processed ASCAT SWI and MODIS snow cover maps used in this study are available upon request. Landuse information is from Copernicus Land Monitoring Service (https://land.copernicus.eu/). MODIS C6 Normalized Difference Vegetation Index (MOD13A3v006) is from NASA EOSDIS Land Processes DAAC (https://doi.org/10.5067/MODIS/MOD13A3.006). The maps of Soil hydraulic properties are from Zhang et al.. (2018, https://doi.org/10.7910/DVN/UI5LCE). The R package of TUWmodel can be downloaded from CRAN (https://cran.r-project.org/web/packages/TUWmodel/index.html).

Author contribution

RT and JP conceived and designed the study, wrote the codes, performed the analyses, and prepared the manuscript. AS and IP prepared the ASCAT soil moisture SWI data used in this study. JK, BS, MK and PV were responsible for the data management, including quality control, processing, and validating. MV and WW provided the analyses related to soil moisture and prepared part of the manuscript. GB supervised the study and contributed to the study design and interpretation of the results. All authors took part in the discussion of the results and revisions of the paper.

Competing interests

The authors declare that they have no conflict of interest.

Acknowledgment

The authors would like to acknowledge financial support provided by the Austrian Science Funds (FWF) as part of the Vienna Doctoral Program on Water Resource Systems (DK W1219-N28) and the Austrian Research Promotion Agency (FFG) through the BMon project (Contract No. 866031). Rui Tong is grateful for the scholarship from China Scholarship Council (CSC).

References

Albergel, C., Rüdiger, C., Pellarin, T., Calvet, J. C., Fritz, N., Froissard, F., Suquia, D., Petitpa, A., Piguet, B., and Martin, E.: From near-surface to root-zone soil moisture using an exponential filter: an assessment of the method based on in-situ observations and model simulations, Hydrol. Earth Syst. Sci., 12, 1323-1337, https://doi.org/10.5194/hess-12-1323-2008, 2008.

Babaeian, E., Sadeghi, M., Jones, S. B., Montzka, C., Vereecken, H., and Tuller, M.: Ground, Proximal, and Satellite Remote Sensing of Soil Moisture, Reviews of Geophysics, 57, 530-616, https://doi.org/10.1029/2018rg000618, 2019.

Bai, P., Liu, X., and Liu, C.: Improving hydrological simulations by incorporating GRACE data for model calibration, Journal of hydrology, 557, 291-304, https://doi.org/10.1016/j.jhydrol.2017.12.025, 2018.

Bergström S: The HBV model—its structure and applications. Report No. 4, Swedish Meteorological and Hydrological Institute, 1992.

BMLRT: ehyd – Hydrographic data and analyses, available at: https://ehyd.gv.at/, last access: 20 Aug 2020.

Brocca, L., Tarpanelli, A., Moramarco, T., Melone, F., Ratto, S. M., Cauduro, M., Ferraris, S., Berni, N., Ponziani, F., Wagner, W., and Melzer, T.: Soil Moisture Estimation in Alpine Catchments through Modeling and Satellite Observations, Vadose Zone Journal, 12, vzj2012.0102, https://doi.org/10.2136/vzj2012.0102, 2013.

Brocca, L., Crow, W. T., Ciabatta, L., Massari, C., Rosnay, P. d., Enenkel, M., Hahn, S., Amarnath, G., Camici, S., Tarpanelli, A., and Wagner, W.: A Review of the Applications of ASCAT Soil Moisture Products, IEEE Journal of Selected Topics in Applied Earth Observations and Remote Sensing, 10, 2285-2306, https://doi.org/10.1109/JSTARS.2017.2651140, 2017.

Chen, F., Crow, W. T., Bindlish, R., Colliander, A., Burgin, M. S., Asanuma, J., and Aida, K.: Global-scale evaluation of SMAP, SMOS and ASCAT soil moisture products using triple collocation, Remote Sensing of Environment, 214, 1-13, https://doi.org/10.1016/j.rse.2018.05.008, 2018.

Chu, W., Gao, X., and Sorooshian, S.: A new evolutionary search strategy for global optimization of high-dimensional problems, Information Sciences, 181, 4909-4927, https://doi.org/10.1016/j.ins.2011.06.024, 2011.

Copernicus Climate Change Service (C3S): C3S ERA5-Land reanalysis. Copernicus Climate Change Service, 2019.

Demirel, M. C., Özen, A., Orta, S., Toker, E., Demir, H. K., Ekmekcioğlu, Ö., Tayşi, H., Eruçar, S., Sağ, A. B., and Sarı, Ö.: Additional value of using satellite-based soil moisture and two sources of groundwater data for hydrological model calibration, Water, 11, 2083, https://doi.org/10.3390/w11102083, 2019.

[Dataset] Didan, K.: MOD13A3 MODIS/Terra vegetation Indices Monthly L3 Global 1km SIN Grid V006 [September 2002 to August 2014], NASA EOSDIS Land Processes DAAC, https://doi.org/10.5067/MODIS/MOD13A3.006, 2015

Duethmann, D., Peters, J., Blume, T., Vorogushyn, S., and Güntner, A.: The value of satellite ‐ derived snow cover images for calibrating a hydrological model in snow ‐ dominated catchments in Central Asia, Water Resources Research, 50, 2002-2021, https://doi.org/10.1002/2013WR014382, 2014.

Dorigo, W., Wagner, W., Albergel, C., Albrecht, F., Balsamo, G., Brocca, L., Chung, D., Ertl, M., Forkel, M., Gruber, A., Haas, E., Hamer, P. D., Hirschi, M., Ikonen, J., de Jeu, R., Kidd, R., Lahoz, W., Liu, Y. Y., Miralles, D., Mistelbauer, T., Nicolai-Shaw, N., Parinussa, R., Pratola, C., Reimer, C., van der Schalie, R., Seneviratne, S. I., Smolander, T., and Lecomte, P.: ESA CCI Soil Moisture for improved Earth system understanding: State-of-the art and future directions, Remote Sensing of Environment, 203, 185-215, https://doi.org/10.1016/j.rse.2017.07.001, 2017.

Duethmann, D., Blöschl, G., and Parajka, J.: Why does a conceptual hydrological model fail to correctly predict discharge changes in response to climate change?, Hydrol. Earth Syst. Sci., 24, 3493-3511, https://doi.org/10.5194/hess-24-3493-2020, 2020.

Efstratiadis, A., and Koutsoyiannis, D.: One decade of multi-objective calibration approaches in hydrological modelling: a review, Hydrological Sciences Journal, 55, 58-78, https://doi.org/10.1080/02626660903526292, 2010.

El Hajj, M., Baghdadi, N., Zribi, M., Rodríguez-Fernández, N., Wigneron, J. P., Al-Yaari, A., Al Bitar, A., Albergel, C., and Calvet, J.-C.: Evaluation of SMOS, SMAP, ASCAT and Sentinel-1 soil moisture products at sites in Southwestern France, Remote Sensing, 10, 569, https://doi.org/10.3390/rs10040569, 2018.

Finger, D., Vis, M., Huss, M., and Seibert, J.: The value of multiple data set calibration versus model complexity for improving the performance of hydrological models in mountain catchments, Water Resources Research, 51, 1939-1958, https://doi.org/10.1002/2014wr015712, 2015.

Franz, K. J., and Karsten, L. R.: Calibration of a distributed snow model using MODIS snow covered area data, Journal of hydrology, 494, 160-175, https://doi.org/10.1016/j.jhydrol.2013.04.026, 2013.

[Dataset] Hall, D. K., and Riggs, G. A.: MODIS/Terra Snow Cover Daily L3 Global 500m Grid, Version 6, [September 2002 to August 2014], Boulder, Colorado USA, NASA National Snow and Ice Data Center Distributed Active Archive Center, https://doi.org/10.5067/MODIS/MOD10A1.006, 2016a.

[Dataset] Hall, D. K., and Riggs, G. A.: MODIS/Aqua Snow Cover Daily L3 Global 500m Grid, Version 6, [September 2002 to August 2014], Boulder, Colorado USA, NASA National Snow and Ice Data Center Distributed Active Archive Center, https://doi.org/10.5067/MODIS/MYD10A1.006, 2016b.

Hahn, S., W. Wagner, S. Steele-Dunne, M. Vreugdenhil, and T. Melzer: Improving ASCAT soil moisture retrievals with an enhanced spatially-variable vegetation parameterization, IEEE Journal of Selected Topics in Applied Earth Observations and Remote Sensing, 2020, submitted.

Han, P., Long, D., Han, Z., Du, M., Dai, L., and Hao, X.: Improved understanding of snowmelt runoff from the headwaters of China's Yangtze River using remotely sensed snow products and hydrological modeling, Remote Sensing of Environment, 224, 44-59, https://doi.org/10.1016/j.rse.2019.01.041, 2019.

Hiebl, J., and Frei, C.: Daily temperature grids for Austria since 1961—concept, creation and applicability, Theoretical and applied climatology, 124, 161-178, https://doi.org/10.1007/s00704-015-1411-4, 2016.

Hiebl, J., and Frei, C.: Daily precipitation grids for Austria since 1961—Development and evaluation of a spatial dataset for hydroclimatic monitoring and modelling, Theoretical and applied climatology, 132, 327-345, https://doi.org/10.1007/s00704-017-2093-x, 2018.

Immerzeel, W., and Droogers, P.: Calibration of a distributed hydrological model based on satellite evapotranspiration, Journal of hydrology, 349, 411-424, https://doi.org/10.1016/j.jhydrol.2007.11.017, 2008.

Kim, H., ~~J. P.~~ Wigneron, ~~S.~~J.-P., Kumar, ~~J.~~S., Dong, ~~W.~~J., Wagner, ~~M.H.~~W., Cosh, ~~D.D.~~M. H., Bosch, ~~C.H.~~D. D., Collins, ~~P.J.~~C. H., Starks, ~~M.~~P. J., Seyfried, ~~V.~~M., and Lakshmi ~~(2020),~~ V.: Global scale error assessments of soil moisture estimates from microwave-based active and passive satellites and land surface models over forest and mixed irrigated/dryland agriculture regions, Remote Sensing of Environment, ~~in press~~251, 112052, https://doi.org/10.1016/j.rse.2020.112052, 2020.

Kavetski, D., Kuczera, G., and Franks, S. W.: Bayesian analysis of input uncertainty in hydrological modeling: 1. Theory, Water Resources Research, 42, https://doi.org/10.1029/2005WR004368, 2006.

Kosugi, K. i.: Three-parameter lognormal distribution model for soil water retention, Water Resources Research, 30, 891-901, https://doi.org/10.1029/93wr02931, 1994.

Kosugi, K. i.: Lognormal Distribution Model for Unsaturated Soil Hydraulic Properties, Water Resources Research, 32, 2697-2703, https://doi.org/10.1029/96wr01776, 1996.

Kundu, D., Vervoort, R. W., and van Ogtrop, F. F.: The value of remotely sensed surface soil moisture for model calibration using SWAT, Hydrological Processes, 31, 2764-2780, https://doi.org/10.1002/hyp.11219, 2017.

Kunnath-Poovakka, A., Ryu, D., Renzullo, L., and George, B.: The efficacy of calibrating hydrologic model using remotely sensed evapotranspiration and soil moisture for streamflow prediction, Journal of hydrology, 535, 509-524, https://doi.org/10.1016/j.jhydrol.2016.02.018, 2016.

Li, Y., Grimaldi, S., Pauwels, V. R., and Walker, J. P.: Hydrologic model calibration using remotely sensed soil moisture and discharge measurements: The impact on predictions at gauged and ungauged locations, Journal of hydrology, 557, 897-909, https://doi.org/10.1016/j.jhydrol.2018.01.013, 2018.

Lo, M. H., Famiglietti, J. S., Yeh, P. F., and Syed, T.: Improving parameter estimation and water table depth simulation in a land surface model using GRACE water storage and estimated base flow data, Water Resources Research, 46, https://doi.org/10.1029/2009WR007855, 2010.

López, P. L., Sutanudjaja, E. H., Schellekens, J., Sterk, G., and Bierkens, M. F.: Calibration of a large-scale hydrological model using satellite-based soil moisture and evapotranspiration products, Hydrology and Earth System Sciences, 21, 3125-3144, https://doi.org/10.5194/hess-21-3125-2017, 2017.

Merz, R., and Blöschl, G.: A regional analysis of event runoff coefficients with respect to climate and catchment characteristics in Austria, Water Resources Research, 45, https://doi.org/10.1029/2008wr007163, 2009.

Merz, R., Parajka, J., and Blöschl, G.: Time stability of catchment model parameters: Implications for climate impact analyses, Water Resources Research, 47, https://doi.org/10.1029/2010wr009505, 2011.

Milzow, C., Krogh, P. E., and Bauer-Gottwein, P.: Combining satellite radar altimetry, SAR surface soil moisture and GRACE total storage changes for hydrological model calibration in a large poorly gauged catchment, Hydrol. Earth Syst. Sci., 15, 1729-1743, https://doi.org/10.5194/hess-15-1729-2011, 2011.

Mousa, B. G., and Shu, H.: Spatial Evaluation and Assimilation of SMAP, SMOS, and ASCAT Satellite Soil Moisture Products Over Africa Using Statistical Techniques, Earth and Space Science, 7, e2019EA000841, https://doi.org/10.1029/2019ea000841, 2020.

Naeimi, V., Scipal, K., Bartalis, Z., Hasenauer, S., and Wagner, W.: An Improved Soil Moisture Retrieval Algorithm for ERS and METOP Scatterometer Observations, IEEE Transactions on Geoscience and Remote Sensing, 47, 1999-2013, https://doi.org/10.1109/TGRS.2008.2011617, 2009.

Naeini, M. R., Yang, T., Sadegh, M., AghaKouchak, A., Hsu, K.-l., Sorooshian, S., Duan, Q., and Lei, X.: Shuffled complex-self adaptive hybrid evolution (SC-SAHEL) optimization framework, Environmental Modelling & Software, 104, 215-235, https://doi.org/10.1016/j.envsoft.2018.03.019, 2018.

Nash, J. E., and Sutcliffe, J. V.: River flow forecasting through conceptual models part I—A discussion of principles, Journal of hydrology, 10, 282-290, https://doi.org/10.1016/0022-1694(70)90255-6, 1970.

Nijzink, R. C., Almeida, S., Pechlivanidis, I. G., Capell, R., Gustafssons, D., Arheimer, B., Parajka, J., Freer, J., Han, D., Wagener, T., van Nooijen, R. R. P., Savenije, H. H. G., and Hrachowitz, M.: Constraining Conceptual Hydrological Models With Multiple Information Sources, Water Resources Research, 54, 8332-8362, https://doi.org/10.1029/2017wr021895, 2018.

Parajka, J., Merz, R., and Blöschl, G.: Estimation of daily potential evapotranspiration for regional water balance modeling in Austria. In 11th International Poster Day and Institute of Hydrology Open Day "Transport of Water, Chemicals and Energy in the Soil - Crop Canopy - Atmosphere System", Slovak Academy of Sciences, Bratislava, 299-306, 2003.

Parajka, J., and Blöschl, G.: Validation of MODIS snow cover images over Austria, Hydrol. Earth Syst. Sci., 10, 679-689, https://doi.org/10.5194/hess-10-679-2006, 2006.

Parajka, J., Naeimi, V., Blöschl, G., Wagner, W., Merz, R., and Scipal, K.: Assimilating scatterometer soil moisture data into conceptual hydrologic models at the regional scale, Hydrol. Earth Syst. Sci., 10, 353-368, https://doi.org/10.5194/hess-10-353-2006, 2006.

Parajka, J., Merz, R., and Blöschl, G.: Uncertainty and multiple objective calibration in regional water balance modelling: case study in 320 Austrian catchments, Hydrological Processes, 21, 435-446, https://doi.org/10.1002/hyp.6253, 2007.

Parajka, J., and Blöschl, G.: The value of MODIS snow cover data in validating and calibrating conceptual hydrologic models, Journal of Hydrology, 358, 240-258, https://doi.org/10.1016/j.jhydrol.2008.06.006, 2008.

Parajka, J., Naeimi, V., Blöschl, G., and Komma, J.: Matching ERS scatterometer based soil moisture patterns with simulations of a conceptual dual layer hydrologic model over Austria, Hydrol. Earth Syst. Sci., 13, 259-271, https://doi.org/10.5194/hess-13-259-2009, 2009.

Pfeil, I., Vreugdenhil, M., Hahn, S., Wagner, W., Strauss, P., and Blöschl, G.: Improving the seasonal representation of ASCAT soil moisture and vegetation dynamics in a temperate climate, Remote Sensing, 10, 1788, https://doi.org/10.3390/rs10111788, 2018.

Rajib, M. A., Merwade, V., and Yu, Z.: Multi-objective calibration of a hydrologic model using spatially distributed remotely sensed/in-situ soil moisture, Journal of hydrology, 536, 192-207, https://doi.org/10.1016/j.jhydrol.2016.02.037, 2016.

Rakovec, O., Kumar, R., Attinger, S., and Samaniego, L.: Improving the realism of hydrologic model functioning through multivariate parameter estimation, Water Resources Research, 52, 7779-7792, https://doi.org/10.1002/2016WR019430, 2016.

Seibert, J.: Multi-criteria calibration of a conceptual runoff model using a genetic algorithm, Hydrol. Earth Syst. Sci., 4, 215-224, https://doi.org/10.5194/hess-4-215-2000, 2000.

Sleziak, P., Szolgay, J., Hlavčová, K., Duethmann, D., Parajka, J., and Danko, M.: Factors controlling alterations in the performance of a runoff model in changing climate conditions, Journal of Hydrology and Hydromechanics, 66, 381, https://doi.org/10.2478/johh-2018-0031, 2018.

Sleziak, P., Szolgay, J., Hlavčová, K., Danko, M., and Parajka, J.: The effect of the snow weighting on the temporal stability of hydrologic model efficiency and parameters, Journal of Hydrology, 583, 124639, https://doi.org/10.1016/j.jhydrol.2020.124639, 2020.

Sutanudjaja, E. H., van Beek, L. P. H., de Jong, S. M., van Geer, F. C., and Bierkens, M. F. P.: Calibrating a large-extent high-resolution coupled groundwater-land surface model using soil moisture and discharge data, Water Resources Research, 50, 687-705, https://doi.org/10.1002/2013wr013807, 2014.

Széles, B., Parajka, J., Hogan, P., Silasari, R., Pavlin, L., Strauss, P., and Blöschl, G.: The ~~added value~~Added Value of ~~different data types~~Different Data Types for ~~calibrating~~Calibrating and ~~testing~~Testing a ~~hydrologic model~~Hydrologic Model in a ~~small catchment~~Small Catchment, Water Resources Research, ~~2020a, In review~~56, e2019WR026153, https://doi.org/10.1029/2019WR026153, 2020.

Széles, B., Parajka, J., Hogan, P., Silasari, R., Pavlin, L., Strauss, P., and Blöschl, G.: Stepwise prediction of runoff using proxy data in a small agricultural catchment. Journal of Hydrology and Hydromechanics, ~~68, X, X-X.~~ 691-11. https://doi~~:~~.org/10.2478/johh-2020-0029, ~~2020b, In press~~2021.

Tong, R., Parajka, J., Komma, J., and Blöschl, G.: Mapping snow cover from daily Collection 6 MODIS products over Austria, Journal of Hydrology, ~~2019, In review~~590, 125548, https://doi.org/10.1016/j.jhydrol.2020.125548, 2020.

Trautmann, T., Koirala, S., Carvalhais, N., Eicker, A., Fink, M., Niemann, C., and Jung, M.: Understanding terrestrial water storage variations in northern latitudes across scales, Hydrol. Earth Syst. Sci., 22, 4061-4082, https://doi.org/10.5194/hess-22-4061-2018, 2018.

Udnæs, H.-C., Alfnes, E., and Andreassen, L. M.: Improving runoff modelling using satellite-derived snow covered area?, Hydrology Research, 38, 21-32, https://doi.org/10.2166/nh.2007.032, 2007.

Viglione, A., Parajka, J., Rogger, M., Salinas, J., Laaha, G., Sivapalan, M., and Blöschl, G.: Comparative assessment of predictions in ungauged basins-Part 3: Runoff signatures in Austria, Hydrology and Earth System Sciences, 17, 2263, https://doi.org/10.5194/hess-17-2263-2013, 2013.

Wagener, T., and Montanari, A.: Convergence of approaches toward reducing uncertainty in predictions in ungauged basins, Water Resources Research, 47, https://doi.org/10.1029/2010WR009469, 2011.

Wagner, W., Lemoine, G., Borgeaud, M., and Rott, H.: A study of vegetation cover effects on ERS scatterometer data, IEEE Transactions on Geoscience and Remote Sensing, 37, 938-948, https://doi.org/10.1109/36.752212, 1999.

Wagner, W., Hahn, S., Kidd, R., Melzer, T., Bartalis, Z., Hasenauer, S., Figa-Saldaña, J., De Rosnay, P., Jann, A., and Schneider, S.: The ASCAT soil moisture product: A review of its specifications, validation results, and emerging applications, Meteorologische Zeitschrift, 22, 5-33, https://doi.org/10.1127/0941-2948/2013/0399, 2013.

Wagner, W., Brocca, L., Naeimi, V., Reichle, R., Draper, C., Jeu, R. d., Ryu, D., Su, C., Western, A., Calvet, J., Kerr, Y. H., Leroux, D. J., Drusch, M., Jackson, T. J., Hahn, S., Dorigo, W., and Paulik, C.: Clarifications on the "Comparison Between SMOS, VUA, ASCAT, and ECMWF Soil Moisture Products Over Four Watersheds in U.S.", IEEE Transactions on Geoscience and Remote Sensing, 52, 1901-1906, https://doi.org/10.1109/TGRS.2013.2282172, 2014.

Wanders, N., Bierkens, M. F. P., de Jong, S. M., de Roo, A., and Karssenberg, D.: The benefits of using remotely sensed soil moisture in parameter identification of large-scale hydrological models, Water Resources Research, 50, 6874-6891, https://doi.org/10.1002/2013wr014639, 2014.

Werth, S., and Güntner, A.: Calibration analysis for water storage variability of the global hydrological model WGHM, Hydrology and Earth System Sciences, 14, 59-78, https://doi.org/10.5194/hess-14-59-2010, 2010.

Zhang, Y., Chiew, F. H., Zhang, L., and Li, H.: Use of remotely sensed actual evapotranspiration to improve rainfall–runoff modeling in Southeast Australia, Journal of Hydrometeorology, 10, 969-980, https://doi.org/10.1175/2009JHM1061.1, 2009.

Zhang, Y., Schaap, M. G., and Zha, Y.: A High-Resolution Global Map of Soil Hydraulic Properties Produced by a Hierarchical Parameterization of a Physically Based Water Retention Model, Water Resources Research, 54, 9774-9790, https://doi.org/10.1029/2018wr023539, 2018.

Table 1. Normalized Difference Snow Index (NDSI) threshold for snow cover mapping from Tong et al. (2019)

Aqua		Jan	Feb	Mar	Apr	May	Jun	Jul	Aug	Sep	Oct	Nov	Dec
below 900 m a.s.l.	non-forest	0.36	0.34	0.36	0.67	0.98	0.97	0.89	0.96	0.84	0.67	0.43	0.41
	coniferous forest	0.17	0.24	0.34	0.50	0.63	0.66	0.79	0.77	0.92	0.47	0.42	0.26
	other forest	0.32	0.29	0.29	0.82	0.70	0.78	0.75	0.89	0.90	0.80	0.47	0.30
over 900 m a.s.l.	non-forest	0.22	0.18	0.28	0.49	0.67	0.91	0.89	0.91	0.71	0.43	0.45	0.26
	coniferous forest	0.20	0.14	0.29	0.49	0.74	0.86	0.82	0.87	0.82	0.49	0.43	0.25
	other forest	0.17	0.12	0.13	0.50	0.83	0.74	0.77	0.58	0.69	0.44	0.46	0.20

Terra		Jan	Feb	Mar	Apr	May	Jun	Jul	Aug	Sep	Oct	Nov	Dec
below 900 m a.s.l.	non-forest	0.32	0.30	0.37	0.57	0.74	0.78	0.82	0.85	0.82	0.52	0.41	0.36
	coniferous forest	0.30	0.19	0.29	0.34	0.72	0.80	0.65	0.93	0.61	0.56	0.31	0.34
	other forest	0.22	0.19	0.29	0.86	0.78	0.64	0.78	0.74	0.65	0.65	0.40	0.31
over 900 m a.s.l.	non-forest	0.21	0.16	0.20	0.44	0.60	0.90	0.77	0.70	0.84	0.54	0.35	0.27
	coniferous forest	0.16	0.12	0.22	0.40	0.65	0.78	0.80	0.76	0.78	0.47	0.37	0.20
	other forest	0.10	0.11	0.10	0.17	0.53	0.16	0.26	0.69	0.67	0.31	0.31	0.22

740

~~Table 2.~~Table 1. **Statistics of the catchment attributes of the 213 catchments in Figure 1 with abbreviation, unit, minimum, maximum, and median. The standard deviations refer to spatial variability within each catchment.**

Information	Attribute	Abbrev.	Unit	Min.	Max.	Median
Size	Area	A	km^2	13.70	6214.00	167.30
Elevation	Mean elevation	MELE	m a.s.l.	353.01	2939.76	1010.73
	Minimum elevation	MiELE	m a.s.l.	200.00	1939.00	561.00
	Maximum elevation	MxELE	m a.s.l.	509.00	3760.00	1861.00
	Elevation range	ER	m	80.00	3072.00	1279.00
	Roughness index (MELE-MiELE)/ER	RI	-	0.15	0.65	0.38
	Mean slope	SL	%	1.74	43.91	18.84
	Mean daily potential global radiation	MGR	$kW \cdot m^{-2} \cdot day$	4.73	6.26	5.19
	Standard deviation of MGR	SDGR	$kW \cdot m^{-2} \cdot day$	0.02	1.10	0.39
Land cover	Coverage of forest	FP	%	0.00	94.59	46.88
	Coverage of agricultural areas	AP	%	0.00	92.86	16.30
	Mean monthly normalized difference vegetation index	MNDVI	-	0.00	0.71	0.60
	Standard deviation of MNDVI	SDNDVI	-	0.02	0.19	0.06
Climate	Mean annual precipitation	MAP	mm	728.13	2301.84	1274.40
	Standard deviation of annual MAP	SDAP	mm	10.79	367.57	124.70
	Mean air temperature	MAT	°C	-2.83	10.30	7.36
	Standard deviation of MAT	SDAT	°C	0.06	3.55	1.26
	Mean annual potential evaporation	MEPI	mm	233.49	740.45	629.57
	Standard deviation of MEPI	SDEPI	mm	4.33	162.07	60.17
	Catchment aridity index (MEPI/MAP)	CAI	-	0.18	0.98	0.47
	Standard deviation of aridity index	SDAI	-	0.01	0.31	0.08
	Proportion of day with temperature below 0 °C	MTL0	-	0.12	0.62	0.20
Soil	Mean field capacity	MFC	$cm^3 \cdot cm^{-3}$	0.29	0.43	0.36
	Standard deviation of MFC	SDFC	$cm^3 \cdot cm^{-3}$	0.01	0.05	0.02
	Mean saturated hydraulic conductivity	MKS	$cm \cdot day^{-1}$	24.88	327.77	161.17
	Standard deviation of MKS	SDKS	$cm \cdot day^{-1}$	6.43	76.03	40.35

745

Table ~~3~~2. Parameters of the hydrologic model (TUWmodel) and ranges used in model calibration. A suitable parameter range may vary by climate and land cover regions and is usually set by expert judgement. The range used here is based on the previous experience of Merz et al. (2011) and Viglione et al. (2013) in the study area.

Parameter	Explanation [Unit]	General Range
SCF	snow correction factor [-]	0.9-1.5
DDF	degree day factor [mm/ °C/day]	0.0-6.0
Ts	threshold temperature below which precipitation is snow [°C]	-3.0-1.0
Tr	threshold temperature above which precipitation is rain [°C]	1.0-3.0
meltT	threshold temperature above which melt starts [°C]	-2.0-2.0
LP	parameter related to the limit for potential evaporation [-]	0.0-1.0
FC	field capacity, i.e., max soil moisture storage [mm]	0-600
beta	the nonlinear parameter for runoff production [-]	0-20
k0	storage coefficient for very fast response [day]	0-2.0
k1	storage coefficient for fast response [day]	2-30
k2	storage coefficient for slow response [day]	30-250
lsuz	threshold storage state, i.e., the very fast response starts if exceeded [mm]	1-100
cperc	constant percolation rate [mm/day]	0.0-8.0
bmax	maximum base at low flows [days]	0.0-30.0
croute	free scaling parameter [$days^2$/mm]	0.0-50.0

750

Table 43. Weights given to runoff, satellite soil moisture (SSM) and satellite snow cover (SSC) in the multiple objective calibration (Eq.1) for different calibration variants. a set of 11 w_Q weights in the range 0.0 and 1.0 is tested for each multiple objective calibration variant. The sum of weights is always 1.0.

Calibration variant	Weight of runoff (w_Q)	Weight of soil moisture (w_{SM})	Weight of snow cover (w_{SC})
Runoff only	$w_Q = 1.0$	$w_{SM} = 0.0$	$w_{SC} = 0.0$
SSM+runoff (Var1)	$w_Q = \{k/10\}_{k=0}^{10}$	$w_{SM} = 1 - w_Q$	$w_{SC} = 0.0$
SSC+runoff (Var2)	$w_Q = \{k/10\}_{k=0}^{10}$	$w_{SM} = 0.0$	$w_{SC} = 1 - w_Q$
SSM+SSC+runoff (Var3)	$w_Q = \{k/10\}_{k=0}^{10}$	$w_{SM} = w_{SC}$	$w_{SC} = w_{SM}$

755

Table 4. Median of runoff (Eq. 2), soil moisture (Eq. 5) and snow cover (Eq. 6) model efficiency obtained from three multiple objective calibration variants: (1) to satellite soil moisture (ASCAT) and runoff (var1); (2) to satellite snow cover (MODIS) and runoff (var2); (3) to satellite soil moisture (ASCAT), satellite snow cover (MODIS) and runoff (var3) in 213 catchments in the ~~5. Median of runoff (Eq. 2), soil moisture (Eq. 5) and snow cover (Eq. 6) model efficiency obtained from three multiple objective calibration variants: (1) to satellite soil moisture (ASCAT) and runoff (var1); (2) to satellite snow cover (MODIS) and runoff (var2); (3) to satellite soil moisture (ASCAT), satellite snow cover (MODIS) and runoff (var3) in 213 catchments in the~~ calibration period 2000-2010.

Weight w_Q	Runoff model efficiency			Soil moisture efficiency			Snow cover efficiency		
	Var1	Var2	Var3	Var1	Var2	Var3	Var1	Var2	Var3
0.00	0.07	0.19	0.18	0.52	0.26	0.45	0.66	0.91	0.91
0.10	0.65	0.60	0.59	0.49	0.30	0.44	0.75	0.91	0.91
0.20	0.71	0.62	0.69	0.47	0.32	0.43	0.80	0.91	0.88
0.30	0.74	0.70	0.73	0.46	0.32	0.43	0.80	0.88	0.86
0.40	0.75	0.74	0.76	0.44	0.31	0.42	0.80	0.87	0.84
0.50	0.76	0.77	0.77	0.43	0.31	0.42	0.80	0.85	0.83
0.60	0.77	0.78	0.78	0.43	0.30	0.40	0.80	0.84	0.82
0.70	0.78	0.78	0.78	0.41	0.30	0.37	0.80	0.82	0.81
0.80	0.78	0.79	0.79	0.39	0.29	0.36	0.80	0.81	0.80
0.90	0.79	0.79	0.79	0.34	0.30	0.32	0.80	0.80	0.80
1.00	0.79	0.79	0.79	0.29	0.29	0.29	0.79	0.79	0.79

765 **Table ~~6. Median of runoff (Eq. 2), soil moisture (Eq. 5) and snow cover (Eq. 6) model efficiency obtained from three multiple objective calibration variants: (1) to satellite soil moisture (ASCAT) and runoff (var1); (2) to satellite snow cover (MODIS) and runoff (var2); (3) to satellite soil moisture (ASCAT), satellite snow cover (MODIS) and runoff (var3) in 213 catchments in the~~ 5. Median of runoff (Eq. 2), soil moisture (Eq. 5) and snow cover (Eq. 6) model efficiency obtained from three multiple objective calibration variants: (1) to satellite soil moisture (ASCAT) and runoff (var1); (2) to satellite snow cover (MODIS) and runoff (var2);**
770 **(3) to satellite soil moisture (ASCAT), satellite snow cover (MODIS) and runoff (var3) in 213 catchments in the validation period 2010-2014.**

Weight	Runoff model efficiency			Soil moisture efficiency			Snow cover efficiency		
	Var1	Var2	Var3	Var1	Var2	Var3	Var1	Var2	Var3
0.00	0.06	0.11	0.17	0.54	0.35	0.48	0.69	0.93	0.93
0.10	0.60	0.57	0.57	0.49	0.43	0.48	0.75	0.93	0.92
0.20	0.67	0.59	0.66	0.51	0.43	0.49	0.81	0.92	0.91
0.30	0.69	0.65	0.70	0.49	0.43	0.49	0.82	0.91	0.88
0.40	0.71	0.70	0.72	0.48	0.42	0.49	0.81	0.89	0.86
0.50	0.72	0.72	0.72	0.48	0.41	0.48	0.82	0.87	0.85
0.60	0.72	0.73	0.73	0.48	0.41	0.47	0.82	0.86	0.84
0.70	0.72	0.73	0.73	0.46	0.40	0.45	0.82	0.84	0.83
0.80	0.73	0.73	0.73	0.45	0.41	0.43	0.82	0.83	0.83
0.90	0.73	0.73	0.73	0.43	0.40	0.42	0.82	0.82	0.82
1.00	0.73	0.73	0.73	0.40	0.40	0.40	0.81	0.81	0.81

Table 7. Kolmogorov-Smirnov p-values testing the similarity of the distribution of catchment attributes across the 213 catchments between those catchments where the runoff model efficiency is improved in the validation period by the inclusion of the soil moisture and snow data in the calibration and those catchments where this is not the case. The null hypothesis that the two samples were drawn from the same distribution is rejected if the p-value is less than the significance level (bold print).

w_Q	**0**	**0.1**	**0.2**	**0.3**	**0.4**	**0.5**	**0.6**	**0.7**	**0.8**	**0.9**
A	0.70	0.34	0.22	0.32	0.15	0.93	**0.05**	0.26	0.46	0.96
MELE	0.23	**0.00**	**0.00**	**0.01**	**0.01**	**0.00**	0.17	**0.03**	0.05	0.25
MiELE	0.27	0.06	0.09	0.20	**0.03**	**0.01**	**0.03**	**0.01**	0.09	0.19
MxELE	0.60	**0.00**	**0.00**	**0.00**	**0.01**	**0.00**	0.23	**0.03**	**0.03**	0.35
ER	0.59	**0.00**	**0.00**	**0.00**	**0.00**	**0.00**	0.47	0.29	**0.02**	0.21
RI	0.49	**0.00**	**0.00**	**0.00**	**0.01**	**0.00**	0.14	**0.03**	**0.03**	0.05
SL	0.11	0.46	0.82	0.37	0.50	0.16	0.18	0.17	0.86	0.81
MGR	0.23	0.73	0.38	0.62	0.05	0.66	0.48	0.98	1.00	0.45
SDGR	0.44	**0.00**	**0.01**	**0.00**	**0.00**	**0.00**	0.11	0.07	**0.02**	0.06
FP	0.29	0.05	**0.05**	0.07	0.40	0.23	0.87	0.80	0.31	0.72
AP	0.20	**0.00**	**0.00**	**0.00**	**0.00**	**0.00**	0.08	**0.02**	**0.02**	0.17
MNDVI	0.71	**0.01**	0.10	**0.03**	**0.04**	**0.04**	**0.05**	**0.04**	0.15	0.21
SDNDVI	0.72	**0.00**	**0.04**	**0.00**	**0.00**	**0.01**	0.49	0.14	**0.01**	0.09
MAP	0.82	**0.00**	0.19	0.08	0.51	**0.01**	**0.03**	0.12	**0.01**	**0.05**
SDAP	0.34	**0.00**	0.05	**0.04**	0.15	0.38	0.93	0.92	**0.03**	0.39
MAT	0.20	**0.00**	**0.00**	**0.00**	**0.01**	**0.00**	0.11	**0.03**	0.10	0.42
SDAT	0.43	**0.00**	**0.01**	**0.01**	**0.00**	**0.01**	0.55	0.16	**0.02**	0.21
MEPI	0.15	**0.00**	**0.00**	**0.00**	**0.00**	**0.00**	0.07	**0.00**	0.13	0.26
SDEPI	0.36	**0.00**	**0.02**	**0.00**	**0.00**	**0.01**	0.63	0.18	**0.01**	0.06
CAI	0.56	**0.00**	**0.01**	**0.00**	0.05	**0.00**	0.20	**0.05**	**0.00**	**0.03**
SDAI	0.78	0.06	**0.03**	**0.04**	**0.01**	0.29	0.38	0.74	0.91	0.82
MTL0	0.20	**0.00**	**0.00**	**0.00**	**0.01**	**0.00**	0.19	**0.02**	0.11	0.31
MFC	0.67	0.14	**0.03**	0.30	0.38	0.08	0.10	0.16	**0.03**	0.10
SDFC	0.14	0.47	0.24	0.56	**0.04**	0.25	0.12	0.69	**0.01**	**0.01**
MKS	0.18	**0.00**	**0.00**	**0.00**	**0.00**	**0.00**	0.17	**0.01**	0.06	0.14
SDKS	0.40	0.19	0.38	0.98	0.07	**0.05**	0.47	0.55	0.11	0.27

780 **Table 8. Same as Table 7, but for the soil moisture model efficiency.**

w_Q	0	0.1	0.2	0.3	0.4	0.5	0.6	0.7	0.8	0.9
A	0.53	0.31	0.18	0.61	0.23	0.26	0.45	0.98	0.98	0.26
MELE	**0.01**	**0.01**	**0.02**	0.07	0.09	**0.05**	0.05	0.70	0.14	0.94
MiELE	**0.01**	0.15	0.13	0.13	0.20	**0.04**	0.05	0.54	0.20	0.74
MxELE	**0.01**	**0.00**	**0.01**	**0.01**	**0.01**	**0.00**	**0.01**	0.13	**0.02**	0.31
ER	0.07	0.08	0.08	**0.03**	**0.04**	**0.02**	0.06	0.22	0.10	0.35
RI	**0.01**	**0.03**	**0.01**	**0.03**	**0.03**	**0.01**	**0.02**	0.38	0.05	0.34
SL	0.32	**0.02**	0.50	0.93	0.35	0.73	0.90	0.45	0.80	0.46
MGR	0.59	0.55	0.69	0.43	0.79	0.25	0.50	0.61	0.49	0.81
SDGR	**0.00**	**0.01**	**0.01**	**0.01**	**0.05**	**0.02**	**0.03**	0.14	0.07	0.17
FP	**0.00**	**0.00**	**0.00**	**0.00**	**0.01**	**0.02**	0.10	0.58	**0.05**	0.35
AP	**0.00**	**0.04**	**0.01**	**0.04**	**0.04**	**0.00**	**0.00**	0.41	0.12	0.32
MNDVI	0.23	**0.01**	0.25	0.89	0.97	0.58	0.36	0.89	0.62	0.67
SDNDVI	0.06	0.63	0.87	0.78	0.62	0.27	0.11	0.69	0.56	0.59
MAP	**0.00**	**0.02**	**0.01**	**0.00**	0.17	**0.01**	**0.03**	0.23	0.07	0.72
SDAP	**0.03**	0.14	0.07	**0.00**	**0.01**	**0.01**	**0.00**	**0.01**	**0.02**	0.07
MAT	**0.01**	**0.02**	**0.01**	**0.03**	**0.05**	**0.02**	**0.02**	0.40	0.12	1.00
SDAT	**0.04**	0.05	0.07	0.08	0.09	0.05	0.07	0.19	0.36	0.22
MEPI	**0.00**	**0.00**	**0.04**	**0.04**	0.06	**0.02**	**0.02**	0.32	0.18	1.00
SDEPI	**0.03**	0.06	**0.03**	**0.04**	**0.05**	**0.03**	**0.05**	0.34	0.17	0.32
CAI	**0.01**	0.05	**0.01**	**0.01**	**0.04**	**0.01**	**0.02**	0.39	0.07	0.82
SDAI	0.44	0.95	0.59	0.79	0.52	0.40	0.44	0.05	0.75	**0.04**
MTL0	**0.01**	**0.02**	**0.02**	0.06	0.07	**0.02**	**0.02**	0.49	0.26	0.83
MFC	**0.00**	**0.00**	**0.00**	**0.01**	**0.04**	**0.01**	**0.04**	0.36	0.09	0.47
SDFC	0.19	0.47	0.34	0.15	0.24	0.05	0.86	0.97	0.16	0.76
MKS	**0.03**	**0.00**	**0.05**	**0.05**	0.06	**0.02**	**0.04**	0.53	0.18	0.76
SDKS	**0.04**	0.19	0.16	**0.04**	0.30	0.08	0.22	0.26	0.42	0.58